Department of AERONAUTICS and ASTRONAUTICS
STANFORD UNIVERSITY

CR-152231

AERODYNAMIC SOUND GENERATION

DUE TO VORTEX-AEROFOIL INTERACTION

PART II

Analysis of the Acoustic Field

by

R. PARTHASARATHY

a n d

K. KARAMCHETI

SEPTEMBER 1972

This work has been sponsored and financially supported by U.S. Army Mobility Research and Development Command, Ames Directorate, under Contract NAS2-6158.

AERODYNAMIC SOUND GENERATION

DUE TO VORTEX-AEROFOIL INTERACTION

PART II

Analysis of the Acoustic Field

by

R. PARTHASARATHY

and

K. KARAMCHETI

SEPTEMBER 1972

This work has been sponsored and financially supported by U.S. Army Mobility Research and Development Command, Ames Directorate, under Contract NAS2-6158.

ACKNOWLEDGEMENT

This work was performed as a part of a research program being conducted in the Department of Aeronautics and Astronautics, Stanford University, and supported by the U.S. Army Mobility Research and Development Command, Ames Directorate, under Contract NAS2-6158.

The authors are thankful to the U.S. Army Mobility Research and Development Command, Ames Directorate, for their support as well as to Messrs Fredric H. Schmitz, Donald A. Boxwell, Rande C. Vause, and Andrew H. Morse for their encouragement and helpful discussions.

TABLE OF CONTENTS

LIST OF ILLUSTRATIONS

Page

NOMENCLATURE

a_0	Ambient speed of sound
a	Radius of the circle in ξ-plane
C	Chord of the Aerofoil
D	Drag force on the aerofoil
F	Field point in the far field
g	Forcing function defined by Eq. (2.4.7)
i	Coordinate along the imaginary axis and = -1
K	Vortex strength
L	Lift force on the aerofoil
M_∞	Mach number
n	Exponent = 3 in Eq. (3.3.16)
p	pressure in the flow field
$\vec{q}$	perturbed velocity vector
R	Distance from the field point to the source point in xy plane
r	radial coordinate
s	source point location
t	Time
$\approx{T}$	Stress tensor
u	x component of the perturbation velocity
U_0	Velocity of the vortex
v	y component of the perturbation velocity
$\vec{V}$	Velocity vector in the flow field
W	Complex potential in ξ-plane
x	x coordinate in the physical plane
y	y coordinate in the physical plane
Z	Complex coordinate
C_p	Pressure coefficient-defined by Eq. (3.4.3)

Greek Symbols

$\alpha = K/U_\infty a$	Nondimensional vortex strength
β	Circulation imposed around the aerofoil
γ	Strength of trailing vortex sheet per unit length
δ	Delta function
ξ	Coordinate in the complex plane
η	Coordinate in the complex plane
θ	Angular coordinate
Γ	Circulation around the aerofoil
ζ	Complex coordinate = $\xi + i\eta$
Φ	Total velocity potential for the flow
φ	Perturbation velocity potential
Ψ	Stream function for the flow
ν	Kinematic viscosity
ρ	Density of the fluid

Subscripts

i,j →	Coordinate indices
0 →	Initial conditions
∞	Infinity conditions

Superscripts

'	Perturbed quantities
~	Nondimensional quantities
-	Refers to complex conjugates

I. INTRODUCTION

This report is concerned with the acoustic field analysis associated with a vortex of modified strength interacting with an airfoil. The general theory of aerodynamic sound has been dealt with in detail in Ref.1. The basic procedure followed here to determine the sound field for the vortex-airfoil interaction has been that due to Lighthill[2]. Lighthill's method of determining the aerodynamic sound field is to first determine the flow field from fluid mechanical principles and then to analyze, independantly of density in the complete flow field, the propagation according to the principles of acoustics.

In a second paper, Lighthill[3] applied his general theory to consider sound generated by turbulence and in particular carried out a detailed theoretical examination of the sound field of a turbulent jet at low subsonic speeds. From the analytical treatment of the aerodynamic sound problem by Lighthill, it was pointed out that solid surfaces even when they are rigid, might well play an important role in the phenomena of sound generation. But a detailed study of the influence of solids boundaries on the mechanism of sound generation was presented by Curle[4]. He extended Lighthill's theory to study the effects of fixed solid boundaries present in a given flow on the sound that is generated aerodynamically and his results distinctly show that the far field sound generated is now due to (i) the quadrupole field distributed in the region where all the fluid fluctuations are dominant, and (ii) to the surface distribution of dipoles, which represents a fluctuating force exerted by the solid boundaries on the flow. This second contribution is due to the presence of the solid boundaries and as pointed out by Curle[4],

the intensity of sound due to the dipoles on the surface becomes increasingly important at low Mach Numbers.

It is clear from the studies of Lighthill and Curle that conventional aerodynamics becomes the starting point for the study of sound field. A particular case of some practical interest is the noise produced by helicopter blades.

The generation of lift by a helicopter in forward flight is accompanied by the development of an aerodynamic flow field of great complexity. Associated with the flight of the helicopter is the characteristic noise called the blade slap or bang. One of the mechanisms generating this noise is explained to be caused by the fluctuating force on the blade due to the interaction with the vortex from another blade. In this particular case of the blade-vortex interaction, the blade interacts with the velocity field of the vortex but does not cut through it. This problem of the blade-vortex interaction has been studied by Sears[5], among other people. Sears has based his analysis on the classical, incompressible, two-dimensional unsteady airfoil theory and further assumed that the part of the blade that produces the noise is many blade-chords in length and that it passes through the field of the vortex lying parallel to and below it. According to this model, the lift on the blade is determined from the gust-entry lift function of Karman and Sears[6] and the fluctuating lift is what is employed to determine the sound generated aerodynamically. A fluctuating force, like the lift on the blade, can be represented according to acoustic terminology as a concentrated dipole, of appropriate strength, at the origin and thus the associated sound field determined.

Widnall[7] has also studied the blade-vortex interaction in connection

with the helicopter noise, by assuming a long blade passing obliquely over a vortex; that is, the interaction being modeled as a two-dimensional airfoil in an oblique gust.

The unsteady lift on the blade due to the blade-vortex interaction has been calculated using linear unsteady aerodynamics in a manner analogous to the the theory of Sears[8] developed purely for two-dimensional interactions. This fluctuating lift force is then employed to calculate the associated sound field.

In the above mentioned studies of Sears[5] and Widhall[7], the far field sound due to the vortex-airfoil interaction is calculated just by determining the fluctuating lift force on the airfoil. The perturbed flow-field around the airfoil, which would constitute the quadrupoles of Lighthill's theory, have been completely ignored. To what extent this is justifiable can only be understood after undertaking a systematic and thorough study of all the individual contributions to the far field sound. Secondly in the model employed by Sears to study the vortex-airfoil interaction, it is assumed that the vortex is held stationary while the airfoil is in uniform rectilinear motion. This is a restriction on the motion of the vortex. A vortex free to move while interacting with the airfoil seems to be a more appropriate model to postulate for the vortex-airfoil interaction. Again, the importance of the free vortex-airfoil interaction can be established after a detailed analysis of the problem from the fluid mechanical principles.

Therefore, with a view to clearly understand the various mechanisms that enter into the determination of the sound field due to the vortex-blade interaction, a free vortex interacting with an airfoil in uniform motion is modeled and analyzed. In Ref.1 classical, incompressible,

inviscid and two-dimensional unsteady flow has been employed for the analysis of the vortex-blade interaction. In that report is presented a complete and detailed analysis of (i) the motion of the free vortex, (ii) the forces acting on the airfoil, (iii) the extent of the perturbed flow field around the airfoil. The determination of the sound field due to all the acoustic sources, not only on the airfoil surface (dipoles) but also due to the ones distributed in the perturbed flow field (quadrupoles) due to the vortex-airfoil interaction, has been presented here. It is important to point out that since inviscid flow assumption has been employed for the study of the vortex-blade interaction, the quadrupoles that have been mentioned above in the perturbed flow field are entirely due to unsteady flow field.

The effects of thickness of the airfoil on the sound radiation are studied by employing a symmetric Joukowski airfoil for the vortex-airfoil interaction.

II. ACOUSTIC FIELD ANALYSIS

2.1 Sound radiation in a Plane

To determine the density fluctuation at any point $\vec{r}_F$, at any time "t" due to a fluctuating fluid flow within volume V_0 bounded by the airfoil surface S and the outer boundary Σ (Sketch No.2) one requires a detailed knowledge of the pressure and velocity fields both on the airfoil surface and the surrounding region V_0. Such information has been obtained in Ref.1 for a two-dimensional, unsteady, motion of vortex interacting with a flat plate airfoil in an incompressible, inviscid potential flow. Hence before the details of the flow field are used to calculate the density fluctuation ρ' at the field point F external to V_0, Eq. (2.4.16) in Ref.1, needs to be simplified to the two-dimensional case. From the assumption that in region V_0, the fluid is incompressible, Eq. (2.4.16) in Ref.1 simplifies to (See Appendix A)

$$\rho'(\vec{r}_F,t) = \left\{ \frac{1}{4\pi a_0^2} \operatorname{div}\operatorname{div} \int_{V_0} \frac{[\tilde{T}]}{r}\, dV_0 \right.$$
$$+ \frac{1}{4\pi a_0^2} \operatorname{div} \int_S \frac{\vec{n} \cdot [\tilde{pI}]}{r}\, dS$$
$$- \frac{\rho_0}{4\pi a_0^2} \int_S \frac{\vec{n} \cdot U_\infty [\partial \vec{v}/\partial x]}{r}\, dS$$
$$\left. - \frac{\rho_0}{4\pi a_0^2} \operatorname{div} \int_S \frac{\vec{n} \cdot [\vec{U}_\infty \vec{q}]}{r}\, dS \right\} \qquad (4.1.1)$$

The last two integrals refer to the contribution from the dipoles distributed on the surface of any arbitrary aerofoil held stationary in a medium where the fluid is in uniform motion with a velocity U_∞ . But specifically, for a flat-plate aerofoil they are identically zero because of the surface boundary condition, namely, $\vec{n} \cdot \vec{V} = 0$ on S . Therefore, for the flat-plate aerofoil in an incompressible flow, Eq. (2.1.1) further reduces to,

$$\rho'(\vec{r}_F,t) = \left\{ \frac{1}{4\pi a_0^2} \text{ div div} \int_{V_0} \frac{[\tilde{T}]}{r} \, dV_0 + \frac{1}{4\pi a_0^2} \text{ div} \int_S \frac{\vec{n} \cdot [p\tilde{I}]}{r} \, dS \right\} \qquad (2.1.2)$$

where any function [G] is defined as

$$[G] = G\left\{ t - \frac{M_\infty x + r}{a_0(1 - M_\infty^2)} \right\}$$

and

$$r = \sqrt{(x_F - x_S)^2 + (1 - M_\infty^2)\left\{(y_F - y_S)^2 + (z_F - z_S)^2\right\}}$$

From Eq. (2.1.2), we observe that the far-field density perturbation $\rho'(\vec{r}_F,t)$ is due to both the volume distribution of quadrupoles and surface dipoles, similar to that expressed by Curle[4] in his paper ,

except that the present results indicate the effect of acoustic dipoles and quadrupoles present in a uniformly moving medium.

In Eq. (2.1.2), the integrands are all three dimensional quantities. They are functions of all the three coordinates (x,y,z). But the fluid mechanics problem of the vortex-aerofoil interaction, from where the above integrands have to be expressed, is solved as a two-dimensional problem. Therefore Eq. (2.1.2) has to be integrated with respect to Z and expressed as a function of x and y only. This is done below.

The field point F is chosen to be in the $z_F = 0$ plane (see sketch below).

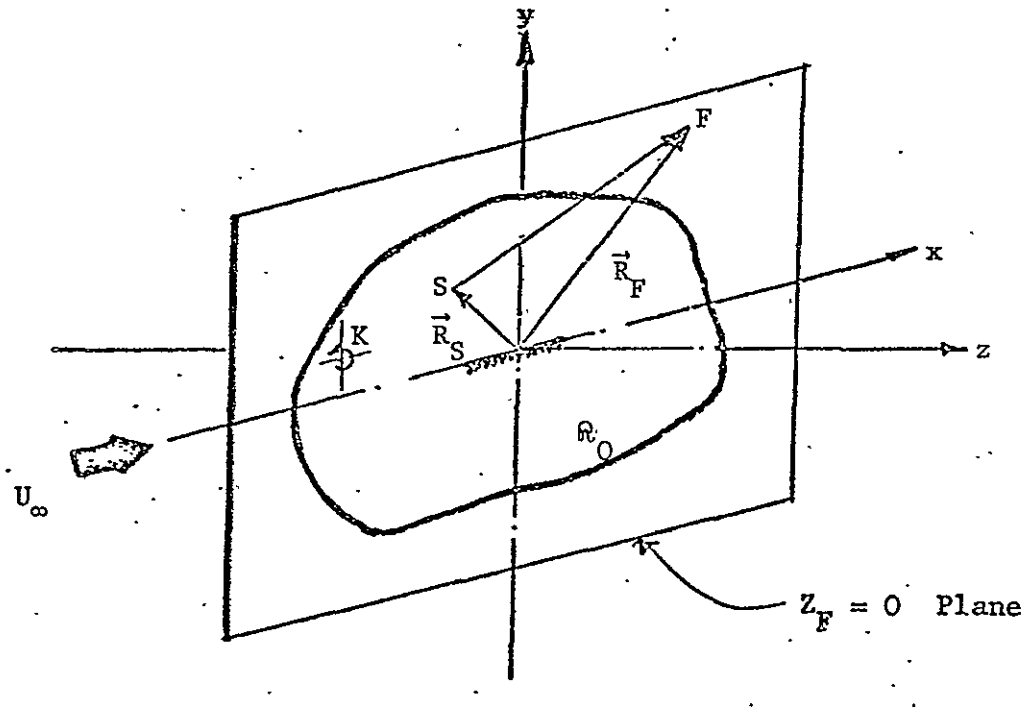

Sketch No. 1 Region of influence of vortex-aerofoil configuration.

All the flow quantities like the perturbed velocity $\vec{q}$ and the pressure p are all only varying in the xy plane and are all independent of z. Hence the density fluctuation ρ' at F which is now a function of x,y and t, is obtained by integrating Eq. (2.1.2) with respect to z_S, from $-\infty$ to $+\infty$. Consider the integral

$$\int_{V_0} \frac{[\tilde{T}]}{r}\, dV_0 = \iint_{R_0} \left\{ \int_{-\infty}^{+\infty} \frac{[T]}{r}\, dz_S \right\} dx_S\, dy_S$$

where

$$r = \sqrt{(x_F - x_S)^2 + (1 - M_\infty^2)\left\{(y_F - y_S)^2 + z_S^2\right\}}$$

Denoting

$$(x_F - x_S)^2 + (1 - M_\infty^2)(y_F - y_S)^2 = R^2 \qquad (2.1.3)$$

it yields for $r = \sqrt{R^2 + (1 - M_\infty^2)\, z_S^2}$

Therefore the integral now becomes,

$$\int_{V_0} \frac{[\tilde{T}]\, dV_0}{r} = 2 \int_{R_0} \int \left\{ \int_{R}^{\infty} \frac{[\tilde{T}]\, dr}{\sqrt{1 - M_\infty^2}\sqrt{r^2 - R^2}} \right\} dx_S\, dy_S \qquad (2.1.4)$$

In the above equation, the integral in the parenthesis, on the right hand side, is defined as

$$\int_R^\infty \frac{[\tilde{T}]\, dr}{\sqrt{r^2 - R^2}} = \int_R^\infty \int_{-\infty}^{+\infty} \frac{\tilde{T}(R,\tau)\, \delta\left(t-\tau - \dfrac{r + M_\infty x}{a_0(1 - M_\infty^2)}\right)}{\sqrt{r^2 - R^2}}\, dr\, d\tau$$

$$= \int_{-\infty}^{\infty} \frac{\tilde{T}(R,\tau)\, d\tau}{\sqrt{\left\{a_0(1 - M_\infty^2)(t - \tau) - M_\infty x\right\}^2 - R^2}} \qquad (2.1.5)$$

Note that the above integral exists only for

$$\tau = \left\{ t - \frac{R + M_\infty x}{a_0(1 - M_\infty^2)} \right\}$$

because the signal that the observer at "F" receives at time "t" is only that originated at

$$\tau = \left\{ t - \frac{R + M_\infty x}{a_0(1 - M_\infty^2)} \right\}$$

and for all other τ , $\tilde{T}(R,\tau) \equiv 0$.

Hence the integral in Eq. (2.1.5) becomes

$$\left[\tilde{T}(R,\tau) \log \left\{ 2\tau - 2 \left(t - \frac{M_\infty x + R}{a_0(1 - M_\infty^2)} \right) + \sqrt{\left\{ t - \tau - \frac{M_\infty x}{a_0(1 - M_\infty^2)} \right\}^2 - \left\{ \frac{R}{a_0(1 - M_\infty^2)} \right\}^2} \right\} \right]$$

$$= \frac{1}{a_0(1 - M_\infty^2)} [\tilde{T}(R,\tau)] \log \left\{ 2R/a_0(1-M_\infty^2) \right\} \qquad (2.1.6)$$

where

$$[\tilde{T}(R,\tau)] = \tilde{T}\left(R,\tau = t - \frac{M_\infty x + R}{a_0(1 - M_\infty^2)}\right) \tag{2.1.7}$$

Hence from Eqs. (2.1.6) and (2.1.7), we have

$$\int_{V_0} \frac{[\tilde{T}]\, dV_0}{r} = \frac{2}{a_0(1 - M_\infty^2)^{3/2}} \iint_{R_0} [\tilde{T}(x_S,y_S)] \log R_1 \, dx_S \, dy_S \tag{2.1.8}$$

where

$$R = \sqrt{(x_F - x_S)^2 + (1 - M_\infty^2)(y_F - y_S)^2}$$

and

$$R_1 = 2R/a_0(1 - M_\infty^2)$$

Similarly in Eq. (4.1.2), the surface integral becomes

$$\int_S \frac{\vec{n} \cdot [p\tilde{I}]}{r} dS = \frac{1}{a_0(1 - M_\infty^2)} \int \vec{n} \cdot [p\tilde{I}] \log R_1 \, dx_S \tag{2.1.9}$$

Therefore, the density fluctuation $\rho'(x_F,y_F,t)$ is given by

$$\rho'(x_F,y_F,t) = \frac{1}{2\pi\, a_0^3(1 - M_\infty^2)^{3/2}} \left\{ \text{div div} \iint_{R_0} [\tilde{T}] \log R_1 \, dx_S \, dy_S \right.$$

$$\left. + \text{div} \int \vec{n} \cdot [p\tilde{I}] \log R_1 \, dx_S \right\} \tag{2.1.10}$$

where

$$\tilde{\tilde{T}} = \rho_0 \vec{q}\,\vec{q} + p\tilde{I} - a_0^2 \rho\, \tilde{I}$$

$$[G] = G\left(t - \frac{M_\infty x + R}{a_0(1 - M_\infty^2)}\right)$$

$$R = \sqrt{(x_F - x_S)^2 + (y_F - y_S)^2(1 - M_\infty^2)}$$

and

$$R_1 = 2R/a_0(1 - M_\infty^2)$$

Furthermore since the fluid fluctuations responsible for the aerodynamic sound generation are solved assuming the flow in region R_0 to be incompressible, it would seem reasonable to identify the sound propagation region, that is the region external to R_0 in the xy-plane, also as one of low Mach number. Therefore the retarded quantities now become

$$[G] \cong G\left(t - \frac{R}{a_0}\right)$$

where

$$R = \sqrt{(x_F - x_S)^2 + (y_F - y_S)^2} \quad . \quad (2.1.11)$$

In the region external to R_0 in the xy plane, (Sketch No. 1), sound is propagating in a uniformly moving medium. In this region the pressure and density are related by

$$p'(x_F, y_F, t) = a_0^2 \rho'(x_F, y_F, t) \qquad (2.1.12)$$

Thus the pressure fluctuation at point F is given by,

$$p'(x_F,y_F,t) = \left\{ \frac{1}{2\pi\, a_0} \text{ div div} \iint_{R_0} [\tilde{T}] \log R_1 \, dx_S \, dy_S + \frac{1}{2\pi\, a_0} \text{ div} \int \vec{n} \cdot [\tilde{p\bar{I}}] \log R_1 \, dx_S \right\} \quad (2.1.13)$$

where assuming that M_∞ is small, we obtain

$$[\tilde{T}] = \tilde{T}(t - R/a_0)$$

$$R = \sqrt{(x_F - x_S)^2 + (y_F - y_S)^2} \quad (2.1.14)$$

and $$R_1 = 2R/a_0$$

2.2 Far Field Simplification

Any quantity [G] is defined to be a quantity G referred to its value at the retarded time $(t - R/a_0)$. Thus

$$\frac{\partial}{\partial x_i}\left\{ [G] \log R_1 \right\} = \left\{ \frac{1}{R_1}\frac{\partial R_1}{\partial x_i} [G] - \frac{\log R_1}{a_0}\left[\frac{\partial G}{\partial t}\right]\frac{\partial R}{\partial x_i} \right\} \quad (2.2.1)$$

Hence for low Mach number flows,

$$\frac{\partial}{\partial x_i}\left\{ [G] \log R_1 \right\} \simeq \left\{ \frac{[G]}{R} - \frac{\log R_1}{a_0}\left[\frac{\partial G}{\partial t}\right] \right\}\frac{\partial R}{\partial x_i} \quad (2.2.2)$$

Out of the two terms in the curly brackets in the above equation, for large distances away from the origin, that is, for large R, the first term becomes smaller as compared to the second term. In fact, this is what defines a "radiation field". Thus in the far field,

$$\frac{\partial}{\partial x_i}\left\{ [G] \log R_1 \right\} \simeq -\frac{\log R_1}{a_0}\left[\frac{\partial G}{\partial t}\right]\frac{\partial R}{\partial x_i} \quad (2.2.3)$$

where

$$\frac{\partial R}{\partial x_i} = -\frac{R_{Fi} - R_{Si}}{R} \tag{2.2.4}$$

and $$R = \sqrt{(x_F - x_S)^2 + (y_F - y_S)^2} \quad .$$

Therefore we obtain

$$\frac{\partial}{\partial x_i}\left\{[G] \log R_1\right\} = + \frac{(R_{Fi} - R_{Si}) \log R}{a_0 R}\left[\frac{\partial G}{\partial t}\right] \tag{2.2.5}$$

Similarly we have,

$$\frac{\partial^2}{\partial x_i \partial x_j}\left\{[G_{ij}] \log R_1\right\} = \left\{\frac{(R_{Fi} - R_{Si})(R_{Fj} - R_{Sj}) \log R_1}{a_0^2 R^2}\left[\frac{\partial^2 G_{ij}}{\partial t^2}\right]\right.$$

$$\left. - \frac{2(R_{Fi} - R_{Si})(R_{Fj} - R_{Sj})}{a_0 R}\left[\frac{\partial G_{ij}}{\partial t}\right]\right\} \tag{2.2.6}$$

Thus Eq. (2.1.13) can now be written as

$$p'(x_F, y_F, t) = \left\{\frac{1}{2\pi a_0}\iint_{R_0}\left\{\frac{(R_{Fi} - R_{Si})(R_{Fj} - R_{Sj})}{a_0^2 R^2}\left[\frac{\partial^2 T_{ij}}{\partial t^2}\right] \log R_1\right.\right.$$

$$\left. - \frac{2(R_{Fi} - R_{Si})(R_{Fj} - R_{Sj})}{a_0 R}\left[\frac{\partial T_{ij}}{\partial t}\right]\right\} dx_S\, dy_S$$

$$\left. + \frac{1}{2\pi a_0}\int_S n_i \frac{(R_{Fi} - R_{Si})}{a_0 R}\left[\frac{\partial p}{\partial t}\right] \log R_1\, dx_S\right\} \tag{2.2.7}$$

Note that all the quantities in the above equation are referred to the "retarded time". The pressure perturbations measured at the field point F (coordinates $\vec{R}_F$) at the instant of time 't' are actually the ones emitted by the source at S (coordinates $\vec{R}_S$) at an earlier time

$$t - \frac{|\vec{R}_F - \vec{R}_S|}{a_0}$$

where a_0 is the uniform speed of sound propagation. The definition of the term "far field" always refers to points, whose distance from the source, $|\vec{R}_F - \vec{R}_S|$ is much greater than the largest wavelength of the propagating sound wave.

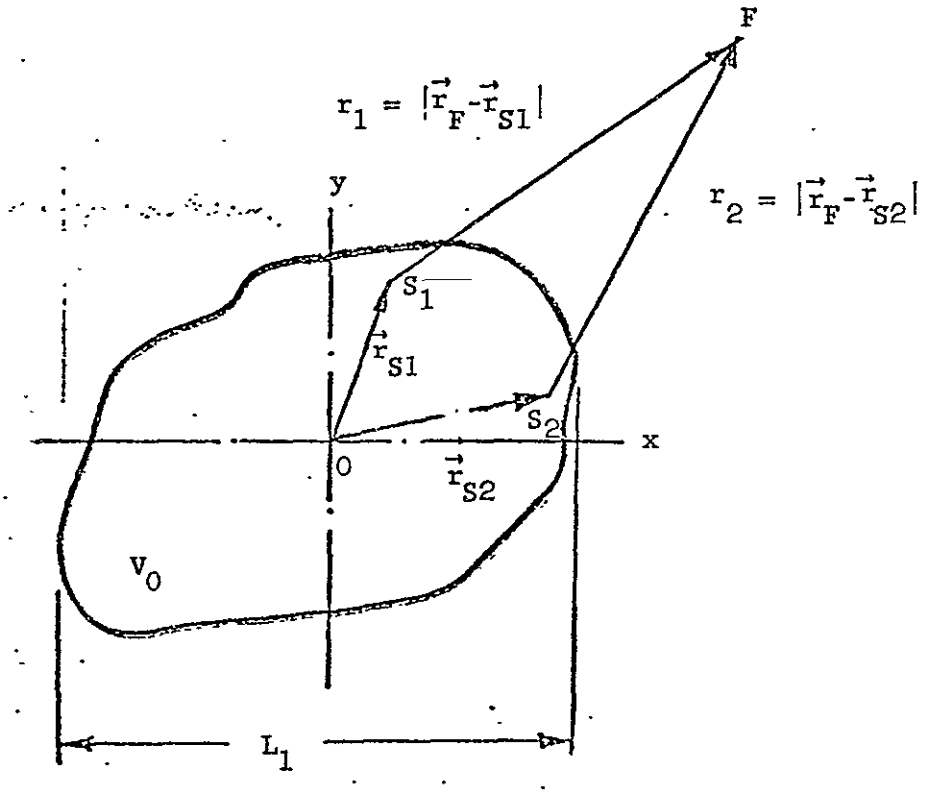

SKETCH No. 2

Referring to the sketch above, let L_1 refer to some maximum characteristic dimension of the region V_0. Consider a point in the far field F where the observer is located and the distance $|\vec{r}_F|$ is much greater than L_1. Consider two source points at S_1 and S_2 within region V_0. Retarded time for the source S_1 is

$$\tau_1 = \left\{ t - \frac{|\vec{r}_F - \vec{r}_{S1}|}{a_0} \right\}$$

and for the source S_2 is

$$\tau_2 = \left\{ t - \frac{|\vec{r}_F - \vec{r}_{S2}|}{a_0} \right\}$$

Hence

$$\Delta\tau = \tau_1 - \tau_2 = \frac{1}{a_0} \left\{ |\vec{r}_F - \vec{r}_{S2}| - |\vec{r}_F - \vec{r}_{S1}| \right\}$$

$$= \frac{S_2S_1}{a_0}$$

Therefore

$$\Delta\tau = \frac{S_2S_1}{a_0} \leq \frac{L_1}{a_0} \quad . \qquad (2.2.8)$$

This means that the time difference in the two signals reaching the observer is at best equal to the time taken for the signals to travel the maximum characteristic distance in the region V_0.

Consider now the time scale of the fluid fluctuations in the flow field in V_0 . The flow velocity is $\vec{V}$. This can be approximated to be the free stream velocity, $\vec{U}_\infty$ for discussion here. Hence the time scale of fluid fluctuations is of the order L_1/U_∞

$$\tau_F = \text{Time scale of fluid fluctuations in } V_0 = L_1/U_\infty \quad . \tag{2.2.9}$$

Thus

$$\frac{\Delta\tau}{\tau_F} \approx \frac{L_1/a_0}{L_1/U_\infty} = M_\infty \tag{2.2.10}$$

Therefore, if the Mach number of the flow is low $(M_\infty \ll 1)$, all the fluctuations in region V_0 will more or less reach the observer at the same time. Thus for low Mach number flows it seems reasonable to ignore the retarded time. Hence Eq. (2.2.7) now becomes

$$p'(x_F,y_F,t) = \left\{ \frac{1}{2\pi a_0} \iint_{R_0} \left\{ \frac{(R_{Fi} - R_{Si})(R_{Fj} - R_{Sj}) \log R_1}{a_0^2 R^2} \left(\frac{\partial^2 T_{ij}}{\partial t^2} \right) - \frac{2(R_{Fi} - R_{Si})(R_{Fj} - R_{Sj})}{a_0 R} \left(\frac{\partial T_{ij}}{\partial t} \right) \right\} dx_S \, dy_S \right.$$
$$\left. + \frac{1}{2\pi a_0} \int_S n_i \frac{(R_{Fi} - R_{Si}) \log R_1}{a_0 R} \left(\frac{\partial p}{\partial t} \right) dx_S \right\} \tag{2.2.11}$$

Defining the following non-dimensional quantities

$$\tilde{p}' = \frac{p'}{\frac{1}{2}\rho_0 U_\infty^2} \quad ; \quad \tilde{T}_{ij} = \frac{T_{ij}}{\frac{1}{2}\rho_0 U_\infty^2} \quad ; \quad \tilde{R}_1 = 2 M_\infty \tilde{R} \quad ;$$

$$\tilde{R} = \frac{R}{a} \quad , \quad \tilde{t} = \frac{U_\infty t}{a} \quad \text{and} \quad a = C/4 \quad .$$

and expressing $$\tilde{p}'(\tilde{x}_F, \tilde{y}_F, \tilde{t}) = \tilde{p}_V' + \tilde{p}_S' \qquad (2.2.12a)$$

we have, after substituting in Eq. (2.2.11), the following;

$$\tilde{p}_V'(\tilde{x}_F, \tilde{x}_F, \tilde{t}) = \frac{M_\infty^2}{2\pi} \iint_{R_0} \left\{ \frac{M_\infty (\tilde{R}_{Fi} - \tilde{R}_{Si})(\tilde{R}_{Fj} - \tilde{R}_{Sj}) \log \tilde{R}_1}{\tilde{R}^2} \left(\frac{\partial^2 \tilde{T}_{ij}}{\partial \tilde{t}^2} \right) \right.$$

$$\left. - \frac{2(\tilde{R}_{Fi} - \tilde{R}_{Si})(\tilde{R}_{Fj} - \tilde{R}_{Sj})}{\tilde{R}} \left(\frac{\partial \tilde{T}_{ij}}{\partial \tilde{t}} \right) \right\} d\tilde{x}_S \, d\tilde{y}_S \qquad (2.2.12b)$$

and

$$\tilde{p}_S'(\tilde{x}_F, \tilde{y}_F, t) = \frac{M_\infty^2}{2\pi} \int_S n_i \frac{(\tilde{R}_{Fi} - \tilde{R}_{Si}) \log \tilde{R}_1}{\tilde{R}} \left(\frac{\partial \tilde{p}}{\partial \tilde{t}} \right) d\tilde{x}_S \qquad (2.2.12c)$$

From Eq. (2.2.12), the term p_V' refers to the pressure propagated into the far field due to the unsteady fluid fluctuations $\tilde{T}_{ij}$ within the region R_0 . Then this is what Lighthill[2] identifies as the quadrupole effect. Similarly p_S' is due to the distribution of the singularities on the surface. As Curle[4] points out, these are surface distribution of dipoles and thus p_S' is then the dipole effect.

Furthermore consider the term p'_S in Eq. (2.2.12). It is

$$\tilde{p}'_S(x_F,y_F,t) = \frac{M_\infty^2}{2\pi}\int_S n_i \frac{\tilde{R}_{Fi} - \tilde{R}_{Si}}{\tilde{R}} \log \tilde{R}_1 \left(\frac{\partial \tilde{p}}{\partial \tilde{t}}\right) dx_S \quad .$$

Considering the maximum characteristic dimension of the aerofoil and comparing it with the location of F, the field point, it is in order to assume $R_{Si} \ll R_{Fi}$. Therefore, now

$$\tilde{p}'_S(\tilde{x}_F,\tilde{y}_F,t) \simeq \frac{M_\infty^2}{2\pi} \frac{\tilde{R}_{Fi} \log \tilde{R}_{F_1}}{\tilde{R}_{F_1}} \int_S n_i \left(\frac{\partial \tilde{p}}{\partial \tilde{t}}\right) dx_S$$

$$= \frac{M_\infty^2}{2\pi} \frac{\tilde{R}_{Fi} \log \tilde{R}_{F_1}}{\tilde{R}_{F_1}} \frac{\partial \tilde{P}_i}{\partial \tilde{t}} \qquad (2.2.13)$$

where

$$\tilde{P}_i(\tilde{t}) = \int_S n_i \, \tilde{p} \, dx_S \qquad (2.2.14)$$

= total resultant force exerted upon the fluid by the solid boundaries

$$\tilde{R}_{F1} = 2 M_\infty \tilde{R}_F \quad , \quad \tilde{R}_F^2 = \tilde{x}_F^2 + \tilde{y}_F^2 \qquad (2.2.15)$$

and n_i the surface normal is independent of time.

Therefore $\partial \tilde{P} / \partial \tilde{t}$ is the time rate of change of the resultant force, which from acoustics represents an equivalent dipole. As mentioned in the earlier chapters, the study of sound field just by the knowledge of the time varying force alone, completely ignores the effect of the quadrupoles in the region R_0. The validity or otherwise of such an assumption can be established by computing the sound field from Eq. (2.2.12).

4.3 Computation of the Sound Field

(a) In Ref.1, where the analysis of the flow field is described, the forces acting on the airfoil, namely, the lift and drag forces, due to the motion of the vortex, have been calculated and shown in Figs. 1 and 2. As is pointed out in the preceding section, from an acoustic standpoint, the time varying forces can be easily represented as dipoles of appropriately varying strength. Hence the pressure fluctuation propagated to the field point F due to these fluctuating forces, is given from Eq. (2.2.13) as

$$\tilde{p}'_S(\tilde{x}_F,\tilde{y}_F,\tilde{t}) = \frac{M_\infty^2}{2\pi} \frac{\tilde{R}_{Fi} \log \tilde{R}_{F_1}}{\tilde{R}_{F_1}} \frac{\partial \tilde{P}_i}{\partial \tilde{t}}$$

where $\tilde{P}_i(t)$ = time varying force. Hence the pressure signal, due to the fluctuating lift and drag forces, is

$$\tilde{p}'_S(\tilde{x}_F,\tilde{y}_F,\tilde{t}) = \frac{M_\infty^2}{2\pi} \frac{\log \tilde{R}_{F_1}}{\tilde{R}_{F_1}} \left\{ \tilde{x}_F \frac{\partial \tilde{D}}{\partial \tilde{t}} + \tilde{y}_F \frac{\partial \tilde{L}}{\partial \tilde{t}} \right\} \quad . \qquad (2.3.1)$$

From Fig. 3, it is easily observed that

$$\frac{\partial \tilde{D}}{\partial \tilde{t}} \ll \frac{\partial \tilde{L}}{\partial \tilde{t}} \quad .$$

Therefore neglecting $\partial\tilde{D}/\partial\tilde{t}$ with respect to $\frac{\partial \tilde{L}}{\partial \tilde{t}}$, we obtain from Eq. (2.3.1) the following simpler form,

$$\tilde{p}'_S(\tilde{x}_F,\tilde{y}_F,\tilde{t}) \simeq \frac{M_\infty^2}{2\pi} \frac{\tilde{y}_F \log \tilde{R}_{F_1}}{\tilde{R}_{F_1}} \left(\frac{\partial \tilde{L}}{\partial \tilde{t}} \right) \qquad (2.3.2)$$

Expressing in polar coordinates,

$$\tilde{p}'_S(\tilde{R}_F,\theta_F,\tilde{t}) \simeq \frac{M_\infty^2}{2\pi} \sin\theta_F \log \tilde{R}_{F_1} \left(\frac{\partial \tilde{L}}{\partial \tilde{t}} \right) \qquad (2.3.3)$$

The lift force $\tilde{L}$ has been computed for the non-dimensional vortex strength, $\alpha = 1.0$, for a flow velocity of $U_\infty = 200$ ft/sec past the flat-plate aerofoil of chord $C = 2$ ft. At sea level conditions, this corresponds to a Mach number flow of $M_\infty = .18$. The field point F is chosen 25 chord lengths away so that $\tilde{R}_F = 100$. From Eq. (2.3.3) it can be seen that $\tilde{p}'_s$ is a maximum at $\theta_F = \pi/2$. The time variation of $\tilde{p}'_s$ for the above situation is shown in Fig. 4. It is observed that a peak value of this $\tilde{p}'_s$ at $\theta_F = \pi/2$ occurs at $\tilde{t} = 50$, that is, at a time when the vortex has moved right above the aerofoil. The important result to be noticed is that the free vortex motion predicts nearly twice as much peak value for $\tilde{p}'_s$ as the constrained vortex thereby emphasizing the importance of the vortex-aerofoil mutual interactions.

(b) From the details of the flow field computation shown in Fig. 5, for the given value of $\alpha = 1.0$, it is found that all the fluid fluctuations, have decayed to the so called acoustic level at a distance of approximately 15 chord lengths away from the origin. In fact the value of C_p, at $\theta_F = \pi/2$ and $\tilde{R}_F = 60$ (15 C) is about 0.05. Therefore for sound field computational purposes, the region R_0 is taken to be a circle of radius equal to 15 chord lengths ($\tilde{R}_F = 60$). Thus, shown in Fig. 6, is a detail of the flow configuration adopted for computational purposes.

One important thing to mention here is, that our analysis, the vortex considered, is a point vortex. It is well known that a point vortex gives rise to a singularity at its center. Therefore, in our problem, the vortex has to be isolated from the rest of the flow field by a small circle of radius ϵ_0.

The effect of the vortex on the flow field is felt strongly when it is closest to the aerofoil. From the trajectory analysis, it is observed athat at $\tilde{t} = 50$, the vortex is at its closest location to the aerofoil. The absolute value of the fluid velocity V , around the neighborhood of the vortex, has been computed from Eq. (3.3.28) for various values of ϵ_0 and shown in Fig. 7 . From these results, a choice of $\tilde{\epsilon}_0 = \frac{\epsilon_0}{a} = 1.0$ was made for computational purposes.

(c) From Eq. (2.2.12), the pressure contributions $\tilde{p}'_V$ and $\tilde{p}'_S$ are evaluated numerically in the compex ζ plane as follows. The integrands are expressed in terms of the flow field details in Appendix D. At time $\tilde{t} = 0$, the vortex of strength $\alpha = 1.0$, is at $\tilde{\xi}_0 = -50$ and $\tilde{\eta}_0 = +2$. All the flow quantities like the velocity and pressure are evaluated, as explained in the earlier chapter. These quantities are then employed to evaluate the double integral $\tilde{p}'_V$ and the line integral $\tilde{p}'_S$. First of all the field point F is taken to be at $\theta_F = 0$ and $\tilde{R}_F = 100$. The double integral $\tilde{p}'_V$ is first evaluated for a given $\tilde{R}_S$ and θ_S varying from 0° to 360°, the value of $\tilde{R}_S$ ranging from $\tilde{R}_S = 1.0$ to $\tilde{R}_S = 60$. Then the value of $\tilde{R}_S$ is changed and integration performed with respect to θ_S . The quadrature subroutine is employed to perform the integration with respect to θ_S whereas the "trapezoidal rule" is used to evaluate the integral with respect to $\tilde{R}_S$. Similarly $\tilde{p}'_S$ is evaluated for $\tilde{R}_S = 1.0$. Therefore we now have $\tilde{p}'_V$ and $\tilde{p}'_S$ evaluated at $\tilde{t} = 0$, for $\theta_F = 0$ and $\tilde{R}_F = 100$. At time $\tilde{t} = 1.0$, the vortex advances to a new location and again the above integrals are all evaluated and the procedure repeated

until $\tilde{t} = 100$ is reached. Now for the same $\tilde{R}_F = 100$; but with θ_F changed to $\theta_F = 30^o$, the integrals are evaluated for $\tilde{t} = 0$ to $\tilde{t} = 100$. Thus a detailed computation of the time variation of the pressure fluctuation at different angular locations of the field point F , at a radius $\tilde{R}_F = 100$ is performed and presented in Figs. 8 (a) and 8 (b).

(d) The pressure signal due to both the quadrupole distributions in the region R_0 and the surface distribution of dipoles on the aerofoil, which has been computed in the previous section, should be expressed in the more faimiliar terms in acoustics, namely the intensity of sound I at the field point F and its directional pattern for varying locations of F . From a physical point of view, energy is being continuously propagated by a traveling wave and therefore intensity I of a traveling wave is then the "time average rate at which energy is transported by the wave per unit area," across a surface normal to the direction of propagation. More briefly, intensity is the average power transported per unit area normal to the direction of propagation.

To recapitulate, it is our aim to compute the intensity of the sound field due to the vortex-aerofoil interaction in the space fixed coordinate system (Sketch No. 1) in Ref.1 where the airfoil is in motion in a fluid at rest. From acoustics it is known that the intensity vector $\vec{I}$ and its relation to the fluid flow quantities is given by

$$\vec{I}(R_F) = \frac{\langle p'^2 \rangle}{\rho_0 a_0} \vec{n} \qquad (2.3.4)$$

where

$$\langle p'^2 \rangle = \lim_{(t_2-t_1)\to\infty} \frac{1}{(t_2-t_1)} \int_{t_1}^{t_2} p'^2(R_F,t)\, dt \qquad (2.3.5)$$

p' = pressure fluctuation in the flow

a_0 = constant speed of sound

ρ_0 = constant density of the fluid

and $\vec{n}$ = unit vector normal to the wave front.

Equation (2.3.4) can now be written as,

$$\vec{I}(\tilde{R}_F) = \frac{\rho_0 U_\infty^4}{4a_0} \tilde{I}\, \vec{n} \quad \text{watts/cm}^2 \qquad (2.3.6)$$

where

$$\tilde{I}(\tilde{R}_F) = \langle \tilde{p}'^2(\tilde{R}_F) \rangle \quad . \qquad (2.3.7)$$

The pressure signal $\tilde{p}'$ in the far-field, which is $\tilde{p}' = \tilde{p}'_V + \tilde{p}'_S$, has been computed earlier for different locations of the field point F , for $\tilde{t} = 0$ to $\tilde{t} = 100$. These results are used to determine the non-dimensional intensity $\tilde{I}$.

Intensity $\tilde{I}$ in the far field for $\tilde{R}_F = 100$ and different angular locations θ_F is calculated and shown in Fig. 10.

Because of the large range of intensities over which the ear is sensitive, a logrithmic rather than an arithmetic scale is chosen to define the "intensity level". Therefore the intensity level, "IL" of

a sound wave is defined by the relation

$$IL = 10 \log_{10} (I/I_0) \qquad (2.3.8)$$

where I_0 is a reference intensity. This is taken to be 10^{-16} watts/cm^2 corresponding to the faintest sound wave that can be heard. Intensity levels are expressed in decibels abbreviated as "dB" and shown in Fig. 10a.

From Figs. 8 to 10, where the pressure in the far field and the corresponding intensities have been shown for the vortex-flat plate aerofoil interaction, it is seen that the maximum sound intensity in the far field occurs at $\theta_F = \pi/2$, that is, right when the vortex has moved on top of the aerofoil. The details of the pressure signals at $\theta_F = \pi/2$ are seen in Fig. 9. The volume distribution of quadrupoles contributes nearly 18% of the pressure from that due to the surface distribution of dipoles; this corresponds to a 25% increase in the associated sound intensity, as shown in Fig. 10. The sound intensity with only the concentrated dipole at the origin representing the total forces acting on the aerofoil agrees with the results obtained considering only the distribution of dipoles on the surface. These results can be seen from Figs. 9 and 10. The effect of the quadrupoles is significant in the sense that it has altered the directivity pattern of the sound intensity in the far-field (Fig. 10a). In terms of intensity levels, from Fig. 10b, the dipole distribution on the surface corresponds to 112.3 dB whereas the cumulative effects of both quadrupoles in R_0 and the dipoles on the aerofoil surface correspond to 113.25 dB at $\theta_F = \pi/2$ for $\tilde{R}_F = 100$ and $M_\infty = .18$.

Once again all the results were obtained numerically with the IBM 360 computer. It took a total of 5.5 minutes of execution time for the computer to evaluate the sound intensity in the far field due to both the surface dipole and volume quadrupole effects.

III. THICKNESS EFFECTS ON THE FAR FIELD SOUND

3.1 Flow Field Study

Up till now, the fluid mechanics of the interaction of a vortex with a flat-plate airfoil and the associated sound field have been analyzed. The thickness of the body gives rise to additional mass fluctuations in the fluid flow. As is familiar to all aerodynamicists, such types of mass fluctuations in fluid flow are represented by simple sources and sinks. For closed bodies such as aerofoils, the net source strength representing them in the fluid flow is zero. Hence the source and sink distribution replacing the finite, closed body appear like dipoles to an observer in the far field and therefore the far field sound radiation is dipole-like. As before, the flow field analysis from fluid mechanical principles, is conducted first.

In order to specifically illustrate the effect of thickness on the far field sound and with a view to utilize the complex variable technique that has been employed to study the interaction of the vortex with a flat=plate aerofoil, (Ref.1) a symmetric Joukowski airfoil is employed. The configuration of a vortex of strength K in a uniform stream U_∞, flowing past a symmetric Joukowski airfoil of maximum thickness ratio $\epsilon = h/C$, where h = maximum thickness of the airfoil and C is the airfoil chord, is shown in Fig. 11. From the Joukowski transformation defined by Eq. (3.3.2) in Ref.1, the symmetric airfoil in the z-plane is transformed to a circle of radius a; from Fig. 11 it is seen that the center O_1 of the circle M in the complex ζ-plane,is on the ζ axis but displaced by a distance ϵ from the origin of the

coordinates. The radius a_1 of the circle M is slightly greater than the fundamental length "a" and the circle M , represents the symmetrical aerofoil in the complex ζ-plane. Writing $a_1 = a(1 + \epsilon)$, where ϵ is a small quantity, we obtain for the chord of the aerofoil $4a(1 + \epsilon^2)$. As ϵ is a small quantity $\epsilon^2 \ll 1$ and thus, to a close approximation, the chord of the aerofoil is $C = 4a$ and the trailing edge in the complex plane is represented by $\xi = +a$ or $\xi_1 = a_1$. It is also known that the maximum thickness is at the quarter chord point and the maximum thickness ratio is $h/C = 1.299\epsilon$.

The complex potential $W(\zeta_1)$, for the symmetric aerofoil-vortex configuration in a uniform stream of U_∞ , is given by

$$W(\zeta_1,\zeta_{01},K,U_\infty) = \left\{U_\infty\left(\zeta_1 + \frac{a_1^2}{\zeta_1}\right) + iK\log(\zeta_1 - \zeta_{01}) - iK\log\left(\zeta_1 - \frac{a_1^2}{\bar{\zeta}_{01}}\right) + iK\log\zeta_1 + i\int_{a_1}^{\infty}\gamma(\xi_1)\log(\zeta_1 - \xi_1)\,d\xi_1 - i\int_0^{a_1}\gamma(\xi_1)\log\left(\zeta_1 - \frac{a_1^2}{\xi_1}\right)d\xi_1\right\} . \qquad (3.1.1)$$

The complex velocity $V(\zeta_1)$ is then given by

$$V(\zeta_1,\zeta_{01},K,U_\infty) = \left\{U_\infty\left(1 - \frac{a_1^2}{\zeta_1^2}\right) + \frac{iK}{\zeta_1 - \zeta_{01}} - \frac{iK}{\zeta_1 - a_1^2/\bar{\zeta}_{01}} + \frac{iK}{\zeta_1} + i\int_a^{\infty}\frac{\gamma(\xi_1)d\xi_1}{(\zeta_1 - \xi_1)} - i\int_0^{a}\frac{\gamma(\xi_1)d\xi_1}{(\zeta_1 - a_1^2/\xi_1)}\right\} \qquad (3.1.2)$$

where $\zeta_1 = \zeta + a\epsilon$.

Now the Kutta condition at the trailing edge, $\zeta = +a$ or $\zeta_1 = +a_1$, demands that the velocity $V(\zeta_1 = +a_1)$ be zero, at every instant of time. Defining the following expression for the strength of the trailing vortex sheet $\gamma(\xi,t)$

$$\gamma(\xi,t) = A[\zeta_0(t)]\left[\frac{\xi - a}{(\xi + a)^3}\right]$$

or

$$\gamma(\xi_1,t) = A[\zeta_{01}(t)]\left[\frac{(\xi_1 - a_1)}{\left|\xi_1 + a(1 - \epsilon)\right|^3}\right] \quad ; \quad \xi_1 = \xi + a\epsilon \qquad (3.1.3)$$

and satisfying the Kutta condition at $\xi = +a$ or $\xi_1 = +a_1$, one obtains for

$$A[(\zeta_{01}(t)] = -4a_1^2 K \frac{1 - \epsilon}{(1 + \epsilon)^2} \frac{\zeta_{01} + \bar{\zeta}_{01} - 2a_1}{(\zeta_{01} - a_1)(\bar{\zeta}_{01} - a_1)} \qquad (3.1.4)$$

so that

$$\gamma(\xi_1,t) = -4a_1^2 K \frac{(1 - \epsilon)}{(1 + \epsilon)^2} \frac{\zeta_{01} + \bar{\zeta}_{01} - 2a_1}{(\zeta_{01} - a_1)(\bar{\zeta}_{01} - a_1)} \frac{(\xi_1 - a_1)}{\left[\xi_1 + a(1 - \epsilon)\right]^3} \qquad (3.1.5)$$

where $\zeta_{01} = \zeta_{01}(t)$.

Substituting for $\gamma(\xi_1,t)$, in Eqs. (3.1.2) and (3.1.2) one obtains for the nondimensional complex potential $\tilde{W}(\tilde{\zeta}_1)$ and the complex velocity $\tilde{V}(\tilde{\zeta}_1)$ the following expressions:

$$\tilde{W}(\tilde{\zeta}_1,\tilde{\zeta}_{01})\alpha_1 = \left[\left(\tilde{\zeta}_1 + \frac{1}{\tilde{\zeta}_1}\right) + i\alpha_1 \log(\tilde{\zeta}_1 - \tilde{\zeta}_{01}) - i\alpha_1 \log\left(\tilde{\zeta}_1 - \frac{1}{\tilde{\zeta}_{01}}\right) + i\alpha_1 \log \tilde{\zeta}_1 - i4\alpha_1 \frac{1-\epsilon}{(1+\epsilon)^2} \frac{\tilde{\zeta}_{01}+\tilde{\bar{\zeta}}_{01}-2}{(\tilde{\zeta}_{01}-1)(\tilde{\bar{\zeta}}_{01}-1)} (I_5 - I_6)\right] \qquad (3.1.6)$$

where

$$I_5 = \left\{ \frac{1}{2(\tilde{\zeta}_1 + \tilde{\epsilon})} + \frac{\tilde{\epsilon} - 1 + 2\tilde{\zeta}_1}{2(\tilde{\zeta}_1 + \tilde{\epsilon})^2} \log (1 + \tilde{\epsilon}) + \frac{(\tilde{\zeta}_1 - 1)^2 \log |\tilde{\zeta}_1 - 1|}{2(1 + \tilde{\epsilon})(\tilde{\zeta}_1 + \tilde{\epsilon})^2} \right\} \tag{3.1.7}$$

$$I_6 = \left\{ \frac{(\tilde{\zeta}_1 - 1)^2 \log |\tilde{\zeta}_1 - 1|}{2(1 + \tilde{\epsilon})(\tilde{\epsilon}\tilde{\zeta}_1 + 1)^2} - \frac{\tilde{\zeta}_1^2(\tilde{\epsilon} - 1) + 2\tilde{\zeta}_1}{2(\tilde{\epsilon}\tilde{\zeta}_1 + 1)^2} \log (\tilde{\epsilon}/1 + \tilde{\epsilon}) + \frac{\tilde{\zeta}_1}{2\tilde{\epsilon}(\tilde{\epsilon}\tilde{\zeta}_1 + 1)} + \frac{\tilde{\epsilon} - 1}{2\tilde{\epsilon}^2} \log (1 + \tilde{\epsilon}) - \frac{1}{2\tilde{\epsilon}^2} \right\} , \tag{3.1.8}$$

and

$$\tilde{\epsilon} = \frac{1 - \epsilon}{1 + \epsilon} \quad ; \quad \text{and} \quad \alpha_1 = \frac{\alpha}{1 + \epsilon} . \tag{3.1.9}$$

Also

$$\tilde{V}\left[\tilde{\zeta}_1, \tilde{\zeta}_{01}, \alpha_1\right] = \left[\left(1 - \frac{1}{\tilde{\zeta}_1^2}\right) + \frac{i\alpha_1}{\tilde{\zeta}_1 - \tilde{\zeta}_{01}} - \frac{i\,\alpha_1 \tilde{\zeta}_{01}}{\tilde{\zeta}_1 \tilde{\zeta}_{01} - 1} + \frac{i\alpha_1}{\tilde{\zeta}_1} - i4\alpha_1 \frac{1 - \epsilon}{(1 + \epsilon)^2} \frac{\tilde{\zeta}_{01} + \tilde{\zeta}_{01} - 2}{(\tilde{\zeta}_{01} - 1)(\tilde{\zeta}_{01} - 1)} (I_7 - I_8) \right] \tag{3.1.10}$$

where

$$I_7 = \left\{ \frac{\tilde{\zeta}_1 - 1}{2(1 + \tilde{\epsilon})(\tilde{\zeta}_1 + \tilde{\epsilon})^2} - \frac{1}{2(\tilde{\zeta}_1 + \tilde{\epsilon})^2} + \frac{(\tilde{\zeta}_1 - 1)}{(\tilde{\zeta}_1 + \tilde{\epsilon})^2} \log \left| \frac{\tilde{\zeta}_1 - 1}{1 + \tilde{\epsilon}} \right| \right\} \tag{3.1.11}$$

$$I_8 = \left\{ - \frac{(\tilde{\zeta}_1 - 1)}{2(1+\tilde{\epsilon})(\tilde{\epsilon}\tilde{\zeta}_1 + 1)^2} + \frac{1}{2\tilde{\epsilon}(\tilde{\epsilon}\tilde{\zeta}_1 + 1)^2} - \frac{(\tilde{\zeta}_1 - 1)}{(\tilde{\epsilon}\tilde{\zeta}_1 + 1)^3} \log \left| \frac{\tilde{\epsilon}(\tilde{\zeta}_1 - 1)}{1+\tilde{\epsilon}} \right| \right\} \tag{3.1.12}$$

and as before $\tilde{\epsilon} = \frac{1 - \epsilon}{1 + \epsilon}$.

The velocity of the vortex, at $\tilde{\zeta}_1 = \tilde{\zeta}_{01}$, is calculated as before (Eq. (3.3.25)) in Ref.1, and it is given by

$$\tilde{u}_0(\tilde{\zeta}_{01}, \alpha_1) = \left[\left(1 - \frac{1}{\tilde{\zeta}_{01}^2} \right) - \frac{i\alpha_1 \tilde{\bar{\zeta}}_{01}}{\tilde{\zeta}_{01}\tilde{\bar{\zeta}}_{01} - 1} + \frac{i\alpha_1}{\tilde{\zeta}_{01}} \right.$$

$$\left. - i4\alpha_1 \frac{1 - \epsilon}{(1 + \epsilon)^2} \frac{\tilde{\zeta}_{01} + \tilde{\bar{\zeta}}_{01} - 2}{(\tilde{\zeta}_{01} - 1)(\tilde{\bar{\zeta}}_{01} - 1)} (I_9 - I_{10}) \right] \tag{3.1.13}$$

where

$$I_9 = \left\{ \frac{\tilde{\zeta}_{01} - 1}{2(1 + \epsilon)(\tilde{\zeta}_{01} + \tilde{\epsilon})^2} - \frac{1}{2(\tilde{\zeta}_{01} + \tilde{\epsilon})^2} + \frac{\tilde{\zeta}_{01} - 1}{(\tilde{\zeta}_{01} + \tilde{\epsilon})^3} \log \left| \frac{\tilde{\zeta}_{01} - 1}{1 + \tilde{\epsilon}} \right| \right\} \tag{3.1.14}$$

and

$$I_{10} = \left\{ - \frac{\tilde{\zeta}_{01} - 1}{2(\tilde{\epsilon}\tilde{\zeta}_{01} + 1)^2(\tilde{\epsilon} + 1)} + \frac{1}{2\tilde{\epsilon}(\tilde{\epsilon}\tilde{\zeta}_{01} + 1)^2} - \frac{\tilde{\zeta}_{01} - 1}{(\tilde{\epsilon}\tilde{\zeta}_{01} + 1)^3} \log \left| \frac{\tilde{\epsilon}(\tilde{\zeta}_{01} - 1)}{1 + \tilde{\epsilon}} \right| \right\} \tag{3.1.15}$$

The circulation developed around the aerofoil is given by

$$\Gamma(t) = -\int_{a_1}^{\infty} \gamma(\xi_1, t)\, d\xi_1 \quad .$$

Substituting for $r(\xi_1, t)$ from Eq. (3.1.3), it yields

$$\tilde{\Gamma}(\tilde{t}) = \frac{\Gamma}{K} = \left(\frac{1+\epsilon}{1-\epsilon}\right)\left\{\frac{\tilde{\zeta}_{01} + \tilde{\bar{\zeta}}_{01} - 2}{(\tilde{\zeta}_{01} - 1)(\tilde{\bar{\zeta}}_{01} - 1)}\right\} \qquad (3.1.16)$$

with $\tilde{\zeta}_{01} = \tilde{\zeta}_{01}(\tilde{t})$.

With the velocity field thus being determined, the trajectory of the vortex and the lift force acting on the aerofoil are calculated for a typical case of $\epsilon = 0.10$. As before the strength of the vortex is $\alpha_1 = 1.0$ and the vortex is located at $\tilde{t} = 0$ at $\tilde{\zeta}_{01} = (-50 + i2)$. The trajectory of the vortex and the lift force experienced by the aerofoil are shown in Fig. 13 . A comparison of the lift force experienced by the symmetric aerofoil with that acting on the flat plate aerofoil is shown in Fig. 14 . Also the circulation around the aerofoil for the two different cases is shown in Fig. 12.

It has been noted earlier that the thickness effect or finiteness of the body can be represented by suitable distribution of sources in the flow. It was also observed that the net effect of such sources replacing the body is dipole-like at large distances. From Eq. (2.1.1) far field pressure is given by

$$p'(\vec{r}_F, t) = \frac{1}{4\pi}\left\{\text{div div} \int_{V_0} \frac{[T]}{r}\, dV_0 + \text{div} \int_S \frac{\vec{n} \cdot [p\tilde{I}]}{r}\, dS \right.$$

$$\left. - \rho_0 \int_S \frac{\vec{n} \cdot [U_\infty (\partial \vec{q}/\partial x)]}{r}\, dS - \rho_0 \,\text{div} \int_S \frac{\vec{n} \cdot [\vec{U}_\infty \vec{q}]}{r}\, dS \right\}$$

Upon reducing the above equation to the two-dimensional case of sound radiation in a plane, and by integrating with respect to z (as in the flat-plate case) it yields for the pressure p' the following expression;

$$p'(\vec{R}_F,t) = \frac{1}{2\pi a_0(1 - M_\infty^2)^{3/2}} \left\{ \text{div div} \int_{R_0} [T] \log R_1 \, dR_0 \right.$$

$$+ \text{div} \int_S \vec{n} \cdot [p\tilde{I}] \log R_1 \, dS$$

$$- \rho_0 \int_S \vec{n} \cdot \left[U_\infty \frac{\partial \vec{q}}{\partial x} \right] \log R_1 \, dS$$

$$\left. - \rho_0 \, \text{div} \int_S \vec{n} \cdot [\vec{U}_\infty \vec{q}] \log R_1 \, dS \right\} \qquad (3.1.17)$$

where, as defined earlier,

$$R = \sqrt{(x_F - x_S)^2 + (1 - M_\infty^2)(y_F - y_S)^2} \quad ; \quad R_1 = 2R/a_0(1-M_\infty^2)$$

and

$$[G_1] = G_1 \left(t - \frac{M_\infty x + R}{a_0(1 - M_\infty^2)} \right) .$$

For low Mach number flows, Eq. (3.1.17) simplifies to

$$p'(\vec{R}_F,t) \cong \frac{1}{2\pi a_0}\left\{ \text{div div} \int_{R_0} [T] \log R_1 \, dR_0 \right.$$

$$+ \text{div} \int_S \vec{n} \cdot [\tilde{pI}] \log R_1 \, dS$$

$$- \rho_0 \int_S \vec{n} \cdot \left[U_\infty \frac{\partial \vec{q}}{\partial x}\right] \log R_1 \, dS$$

$$\left. - \rho_0 \, \text{div} \int_S \vec{n} \cdot [\vec{U}_\infty \vec{q}] \log R_1 \, dS \right\} \qquad (3.1.18)$$

where

$$R \simeq \sqrt{(x_F - x_S)^2 + (y_F - y_S)^2} \quad ; \quad R_1 = 2R/a_0$$

and

$$[G_1] = G_1\left(t - \frac{M_\infty + R}{a_0}\right) .$$

From the above equation, the pressure in the far field and thus the sound intensity can be determined, as before.

3.2 Far Field Sound Radiation

In the preceding chapter for the case of the vortex interacting with the flat-plate aerofoil, the analysis of the acoustic field clearly illustrated the significant role played by the quadrupoles

distributed in the volume V_0 enclosing the perturbed flow field. It is our purpose now to study specifically the effect of thickness on the radiated sound to the far field. Therefore we direct our attention only to the surface integrals in Eq. (3.1.18). The first of the three surface integrals, as seen from the earlier chapters, is the effect of the dipoles distributed on the surface of the aerofoil. Even though this integral gives different contribution from that for the flat-plate aerofoil, one can specifically identify the other two surface integrals as definitely due to the thickness of the aerofoil. Therefore, grouping these three surface integrals together and writing them in their nondimensional form it yields

$$\tilde{p}'_S(\tilde{R}_F,\tilde{t}) \simeq \frac{M_\infty^2}{2\pi}\left\{ \int_0^{2\pi} \left(\frac{\tilde{R}_{Fi} - \tilde{R}_{Si}}{\tilde{R}}\right)\left(\frac{\partial \tilde{p}}{\partial \tilde{t}}\right) \log\,(2\,M_\infty\,\tilde{R})d\theta \right.$$

$$+ 2\int_0^{2\pi} \frac{\tilde{R}_{Fi} - \tilde{R}_{Si}}{\tilde{R}} \left(\frac{\partial \tilde{q}_i}{\partial \tilde{t}}\right) \cos\,\theta \log\,(2\,M_\infty\,\tilde{R})\,d\theta$$

$$\left. + 2\int_0^{2\pi} \frac{\tilde{R}_F - \tilde{R}_S}{\tilde{R}}\left(\cos\,\theta\,\frac{\partial \tilde{q}_x}{\partial \tilde{t}} + \sin\,\theta\,\frac{\partial \tilde{q}_y}{\partial \tilde{t}}\right) \log\,(2\,M_\infty\,R)d\theta \right\} \tag{3.2.1}$$

The velocity field components $\tilde{q}_x$, $\tilde{q}_y$ and the pressure distribution $\tilde{p}$ have all been known from the flow field analysis in the earlier section. As in the flat plate case, the above integral is evaluated

for the initial location of the vortex $\tilde{\zeta}_0 = (-50 + i2)$ at $\tilde{t} = 0$ and for all the subsequent locations of the vortex, as it moves along. The results for the pressure in the far field for $\tilde{R}_F = 100$ and for different angular locations θ_F of the field point are all shown in Figs. 15(a) and 15(b) for the specific vortex strength $\alpha = 1.0$. Once again the maximum contribution to the pressure history with time occurs just when the vortex is above the aerofoil. The pressure is a maximum for the field point location of $\theta_F = \pi/2$ for $\tilde{R}_F = 100$.

In Fig. 16 is shown a comparison of the pressure variation with time, for the field point location of $\theta_F = \pi/2$ and $\tilde{R}_F = 100$ computed from a single concentrated dipole model with the one computed from the surface distribution of dipoles. There is a slight difference in the results unlike for the case of the flat-plate aerofoil. This difference can be easily explained from Eq. (3.2.1). The first integral represents the concentrated dipole whereas the effect of thickness is comming from the other two integrals.

In Fig. 17 is shown the comparison of the pressures determined for both the symmetric and flat-plate aerofoil cases, as predicted by the lift force action on the aerofoils. The effect of thickness on the far field is quite evident. It is clearly seen that a 10% thick symmetric aerofoil has increased the peak pressure in the far field by nearly 50% over that predicted for the flat-plate aerofoil. The sound intensity, being proportional to the square of the pressure perturbation, is nearly twice as much for the 10% thick symmetric aerofoil as is for the flat-plate aerofoil. This is shown in Fig. 18. The corresponding intenstity levels are shown in Fig. 19.

VI. SUMMARY AND CONCLUSIONS

A study of the aerodynamic sound produced by a vortex passing past an airfoil in uniform motion is studied.

Following theprocedure proposed by Lighthill to study how aerodynamic flows produce noise, the complete flow field is broadly divided into two separate regions, namely (i) a region of sound generation in the neighborhood of the airfoil, and (ii) a uniform madium at rest where sound is propagated due to the fluid fluctuations in the region around the airfoil.

The vortex-airfoil interaction problem is formulated as a vortex of strength K being released ahead of a flat-plate of chord C at a specific location, at time = 0 . Classical two-dimensional incompressible, inviscid, unsteady potential airfoil theory has been employed to determine (i) the trejectory of the vortex, (ii) the forces acting on the airfoil, and (iii) the complete flow field around the airfoil. This analysis is presented in Ref.1.

The computation of the sound field due to such a fluid mechanics problem is done in two ways: (i) the forces acting on the airfoil, specifically the lift force, from acoustics, is represented as a dipole at the origin and its far-field sound radiation determined; (ii) not only the forces acting on the airfoil but also the fluid fluctuations in the flow around the airfoil are taken into account to compute the far-field sound. The analysis does indicate that the fluid fluctuations in the neighborhood of the airfoil contribute nearly 25 to 30% to the intensity of sound in the far-field.

The effects of thickness of the airfoil on the sound radiation are studied by employing a symmetric Joukowski airfoil interacting

with the free vortex. The increase in the sound intensity in the far-field is nearly twice as much for a 10% thick symmetric airfoil as it is for the flat plate case.

All the numerical computations were performed on IBM-360. It took less than a minute of comuter time to compute the trajectory of the vortex and the free forces acting on the airfoil, whereas the computation of the directivity pattern of the sound intensity in the farfield due to both the surface dipoles and volume distribution of quadrupoles took a total of 5.5 minutes of execution time.

Conclusions

From the results of the acoustic field analysis of the vortex-airfoil interaction, the following conclusions can be drawn; (a) the estimation of the sound generated just by the knowledge of the lift force acting on the airfoil, underestimates the intensity in the far-field. The distribution of quadrupoles in the region around the airfoil makes significant contributions to the sound intensity in the far-field and thus cannot be neglected. Our earlier statements that the far-field sound is due to the cumulative effect of, not only the dipoles distributed on the surface of the airfoil, but also the quadrupoles distributed in the perturbed flow region around the airfoil is well borne out by the results; (b) The effects of thickness on the sound intensity in the far field is illustrated by considering only the dipoles distributed on the airfoil surface. It is observed from the results that a 10% thick symmetric airfoil nearly doubles the sound intensity in the far-field over its value for a flat plate airfoil.

REFERENCES

1. PARTHASARATHY, R., and KARAMCHETI, K., "Aerodynamic Sound Generation due to Vortex-Aerofoil Interaction" - Part I, Sept. 1972
2. LIGHTHILL, M.J., "On Sound Generated Aerodynamically" - Proceedings of the Royal Society, Series A, Vol.211, pp.564-587, 1952.
3. LIGHTHILL, M.J., "Sound Generated Aerodynamically - The Bakerian Lecture", Proceedings of the Royal Society, Series A, Vol.267, pp.148-182, 1962.
4. CURLE, N., "The Influence of Solid Boundaries upon Aerodynamic Sound", Proceedings of the Royal Society, Series A, Vol.231, pp.505-514, 1955.
5. SEARS, W.R., "Aerodynamics, Noise and the Sonic Boom", 1968 Von Karman Lecture, AIAA Journal, Vol.7, No.4, April 1969.
6. VON KARMAN, T., and SEARS, W.R., "Aerofoil Theory for Non-Uniform Motion", Journal of Aero Sciences, Vol.5, No.10, pp.379-390, August 1938.
7. WIDNALL, Sheila, "Helicopter Noise due to Blade-Vortex Interaction", Journal of the Acoustic Society of America, Vol. 50, No.1 (Part 2), pp. 354-366, July 1971.
8. TING, L., and TUNG, C., "Motion and Decay of Vortex in Nonuniform Stream", Physics of Fluids, Vol. 8, No. 6, June 1965.
9. DURAND, W.F., "Aerodynamic Theory" Vol.2, Julius Springer, Berlin, 1935.
10. KARAMCHETI, K., "Ideal Fluid Aerodynamics", John Wiley and Sons, New York, 1966.
11. MILNE-THOMPSON, L.M., "Theoretical Hydrodynamics", The McMillan Co. New York, 1960.

APPENDIX A

A.1 Consider $\mathrm{div}(\rho\vec{q}\,\vec{q} + p\tilde{I})$ in Eq. (2.4.16) in Ref.1. From the continuity and momentum equations, Eqs. (2.4.4) and (2.4.5) in Ref.1, the momentum equation can be written as

$$\left(\frac{\partial}{\partial t} + \vec{U}_\infty \cdot \nabla\right)(\rho\vec{q}) + \mathrm{div}\,\rho\vec{q}\,\vec{q} = -\nabla p \text{ , so that}$$

$$\mathrm{div}(\rho\vec{q}\,\vec{q} + p\tilde{I}) = -\left(\frac{\partial}{\partial t} + \vec{U}_\infty \cdot \nabla\right)(\rho\vec{q})$$

But $$\vec{V} = \vec{U}_\infty + \vec{q} \quad ; \quad U_\infty = \text{constant} \tag{A.1.1}$$

Hence for the incompressible flow considered,

$$\mathrm{div}(\rho\vec{q}\,\vec{q} + p\tilde{I}) = -\rho_0\left(\frac{\partial}{\partial t} + \vec{U}_\infty \cdot \nabla\right)\vec{V}$$

$$= -\left\{\rho_0 \frac{\partial \vec{V}}{\partial t} + \rho_0 \vec{U}_\infty \cdot \nabla\vec{V}\right\} \tag{A.1.2}$$

Therefore $\vec{n} \cdot \mathrm{div}(\rho\vec{q}\,\vec{q} + p\tilde{I})$

$$= -\rho_0 \vec{n} \cdot \frac{\partial \vec{V}}{\partial t} - \rho_0 \vec{n} \cdot (\vec{U}_\infty \cdot \nabla\vec{V})$$

$$= -\rho_0 \frac{\partial}{\partial t}(\vec{n} \cdot \vec{V}) - \rho_0\left(\vec{n} \cdot U_\infty \frac{\partial \vec{V}}{\partial x}\right) \tag{A.1.3}$$

But $\vec{n} \cdot \vec{V} = 0$ on the body surface.

$$\therefore \int_S \frac{\vec{n} \cdot [\mathrm{div}(\rho\vec{q}\,\vec{q} + p\tilde{I})]}{|\vec{r}_F - \vec{r}_S|}\, dS = -\rho_0 \int_S \frac{\left[\vec{n} \cdot U_\infty \frac{\partial \vec{V}}{\partial x}\right]}{|\vec{r}_F - \vec{r}_S|} \tag{A.1.4}$$

A.2 Consider the term $\rho\vec{V}\,\vec{V}$.

Now $\vec{V} = \vec{U}_\infty + \vec{q}$

Hence $\rho\,\vec{V}\,\vec{V} = \rho\vec{V}(\vec{U}_\infty + \vec{q})$

$$= \rho\vec{V}\,\vec{U}_\infty + \rho\vec{V}\,\vec{q}$$

$$= \rho\vec{V}\,\vec{U}_\infty + \rho\vec{U}_\infty\vec{q} + \rho\vec{q}\,\vec{q}$$

Therefore $\rho\vec{q}\,\vec{q} = \rho\vec{V}\,\vec{V} - \rho\vec{V}\,\vec{U}_\infty - \rho\vec{U}_\infty\vec{q}$ (A.2.1)

Hence $$\int_S \frac{\vec{n}\cdot\rho\,\vec{q}\,\vec{q}}{r}\,dS$$

$$= \int_S \frac{\vec{n}\cdot(\rho\vec{V}\,\vec{V} - \rho\vec{V}\,\vec{U}_\infty - \rho\vec{U}_\infty\vec{q})}{r}\,dS$$

$$= \rho_0 \int_S \frac{(\vec{n}\cdot\vec{V})\vec{V} - (\vec{n}\cdot\vec{V})\vec{U}_\infty - (\vec{n}\cdot\vec{U}_\infty)\vec{q}}{r}\,dS$$

$$= -\rho_0 \int_S \frac{(\vec{n}\cdot\vec{U}_\infty)\vec{q}}{r}\,dS \qquad \text{(A.2.2)}$$

because $\vec{n}\cdot\vec{V} = 0$ on S .

$$\therefore \quad \text{div} \int_S \frac{\vec{n}\cdot[\rho\,\vec{q}\,\vec{q}]}{r}\,dS = -\rho_0\,\text{div}\int_S \frac{\vec{n}\cdot[\vec{U}_\infty\vec{q}]}{|\vec{r}_F - \vec{r}_S|}\,dS \qquad \text{(A.2.3)}$$

APPENDIX B

B.1 From Eq. (3.5.4) in Ref.1, the non-dimensional perturbation is given by

$$\tilde{p}' = (p-p_\infty)/\tfrac{1}{2}\rho U_\infty^2)$$

$$= 1 - \tilde{V}^2 - 2\frac{\partial \Phi}{\partial \tilde{t}}$$

$$= 1 - \tilde{V}\,\tilde{\bar{V}} - 2\,\text{Real}\left(\frac{\partial \tilde{W}}{\partial \tilde{t}}\right) \qquad \text{(B.1.1)}$$

Hence the time derivative of $\tilde{p}'$ is given by

$$\frac{\partial p'}{\partial \tilde{t}} = -2\,\text{Re}\left(\tilde{V}\frac{\partial \tilde{\bar{V}}}{\partial \tilde{t}}\right) - 2\,\text{Re}\left(\frac{\partial^2 \tilde{W}}{\partial \tilde{t}^2}\right) \qquad \text{(B.1.2)}$$

and $$\frac{\partial \tilde{W}}{\partial \tilde{t}} = \frac{\partial \tilde{W}}{\partial \tilde{\zeta}_0}\frac{\partial \tilde{\xi}_0}{\partial \tilde{t}} + \frac{\partial \tilde{W}}{\partial \tilde{\bar{\zeta}}_0}\frac{\partial \tilde{\bar{\zeta}}_0}{\partial t}$$

$$= \tilde{U}_0\frac{\partial \tilde{W}}{\partial \tilde{\zeta}_0} + \tilde{\bar{U}}_0\frac{\partial \tilde{W}}{\partial \tilde{\bar{\zeta}}_0} \qquad \text{(B.1.3)}$$

where

$$\tilde{U}_0 = u_0 - iv_0 = \text{complex vortex velocity at } \tilde{\zeta} = \tilde{\zeta}_0$$

and

$$\tilde{\bar{U}}_0 = \text{Complex conjugate of } \tilde{U}_0$$

Similarly we obtain for,

$$\frac{\partial \tilde{W}}{\partial \tilde{t}} = \tilde{U}_0\frac{\partial \tilde{W}}{\partial \tilde{\zeta}_0} + \tilde{\bar{U}}_0\frac{\partial \tilde{W}}{\partial \tilde{\bar{\zeta}}_0} \qquad \text{(B.1.4)}$$

and

$$\frac{\partial^2 \tilde{W}}{\partial \tilde{t}^2} = \left[\left(\tilde{U}_0 \frac{\partial \tilde{U}_0}{\partial \tilde{\zeta}_0} + \tilde{U}_0 \frac{\partial \tilde{\bar{U}}_0}{\partial \tilde{\bar{\zeta}}_0}\right) \frac{\partial \tilde{W}}{\partial \tilde{\zeta}_0} + \left(\tilde{\bar{U}}_0 \frac{\partial \tilde{U}_0}{\partial \tilde{\zeta}_0} + \tilde{U}_0 \frac{\partial \tilde{\bar{U}}_0}{\partial \tilde{\bar{\zeta}}_0}\right) \frac{\partial \tilde{W}}{\partial \tilde{\bar{\zeta}}_0} + \tilde{U}_0^2 \frac{\partial^2 \tilde{W}}{\partial \tilde{\bar{\zeta}}_0^2} + \tilde{\bar{U}}_0^2 \frac{\partial^2 \tilde{W}}{\partial \tilde{\zeta}_0^2} + 2\tilde{U}_0 \tilde{\bar{U}}_0 \frac{\partial^2 \tilde{W}}{\partial \tilde{\zeta}_0 \partial \tilde{\bar{\zeta}}_0}\right] \qquad \text{(B.1.5)}$$

B.2 Again from earlier Eq. (B.1.2), we have

$$\frac{\partial \tilde{p}'}{\partial \tilde{t}} = -\frac{\partial}{\partial \tilde{t}} (\tilde{V} \tilde{\bar{V}}) - 2 \text{ Re} \left(\frac{\partial^2 \tilde{W}}{\partial \tilde{t}^2}\right)$$

Therefore

$$\frac{\partial^2 p'}{\partial \tilde{t}^2} = -\frac{\partial^2}{\partial \tilde{t}^2} (\tilde{V} \tilde{\bar{V}}) - 2 \text{ Re} \left(\frac{\partial^3 \tilde{W}}{\partial \tilde{t}^3}\right) \qquad \text{(B.2.1)}$$

$$\frac{\partial^2}{\partial \tilde{t}^2} (\tilde{V} \tilde{\bar{V}}) = 2 \left|\frac{\partial \tilde{V}}{\partial \tilde{t}}\right|^2 + 2 \text{ Re} \left(\tilde{V} \frac{\partial^2 \tilde{\bar{V}}}{\partial \tilde{t}^2}\right) \qquad \text{(B.2.2)}$$

$$\frac{\partial^2 \tilde{\bar{V}}}{\partial \tilde{t}^2} = \text{conjugate} \left(\frac{\partial^2 \tilde{V}}{\partial \tilde{t}^2}\right) \qquad \text{(B.2.3)}$$

But from Eq. (B.1.3), we obtain

$$\frac{\partial^2 \tilde{V}}{\partial \tilde{t}^2} = \left[\left(\tilde{U}_0 \frac{\partial \tilde{U}_0}{\partial \tilde{\zeta}_0} + \tilde{V}_0 \frac{\partial \tilde{U}_0}{\partial \tilde{\xi}_0} \right) \frac{\partial \tilde{V}}{\partial \tilde{\zeta}_0} + \tilde{U}_0^2 \frac{\partial^2 \tilde{V}}{\partial \tilde{\xi}_0^2} \right.$$

$$+ \left(\tilde{U}_0 \frac{\partial \tilde{V}_0}{\partial \tilde{\zeta}_0} + \tilde{V}_0 \frac{\partial \tilde{V}_0}{\partial \tilde{\xi}_0} \right) \frac{\partial \tilde{V}}{\partial \tilde{\zeta}_0} + \tilde{U}_0^2 \frac{\partial^2 \tilde{V}}{\partial \tilde{\zeta}_0^2}$$

$$\left. + 2\tilde{U}_0 \tilde{V}_0 \frac{\partial^2 \tilde{V}}{\partial \tilde{\zeta}_0 \partial \tilde{\xi}_0} \right] \qquad \text{(B.2.4)}$$

Also

$$\frac{\partial^3 \tilde{W}}{\partial \tilde{t}^3} = \left\{ A_1 \frac{\partial \tilde{W}}{\partial \tilde{\zeta}_0} + A_2 \frac{\partial^2 \tilde{W}}{\partial \tilde{\zeta}_0^2} + A_3 \frac{\partial^3 \tilde{W}}{\partial \tilde{\zeta}_0^3} \right.$$

$$\left. + B_1 \frac{\partial \tilde{W}}{\partial \tilde{\zeta}_0} + B_2 \frac{\partial^2 \tilde{W}}{\partial \tilde{\zeta}_0^2} + B_3 \frac{\partial^3 \tilde{W}}{\partial \tilde{\zeta}_0^3} \right\} \qquad \text{(B.2.5)}$$

where

$$A_1 = \left[\tilde{U}_0 \left(\frac{\partial \tilde{U}_0}{\partial \tilde{\zeta}_0} \right)^2 + \tilde{U}_0^2 \frac{\partial^2 \tilde{U}_0}{\partial \tilde{\zeta}_0^2} + \tilde{U}_0^2 \frac{\partial^2 \tilde{U}_0}{\partial \tilde{\xi}_0^2} \right.$$

$$\left. + 2\tilde{U}_0 \tilde{V}_0 \frac{\partial^2 \tilde{U}_0}{\partial \tilde{\zeta}_0 \partial \tilde{\xi}_0} + \frac{\partial \tilde{U}_0}{\partial \tilde{\zeta}_0} \left\{ \tilde{U}_0 \frac{\partial \tilde{U}_0}{\partial \tilde{\xi}_0} + \tilde{U}_0 \frac{\partial \tilde{U}_0}{\partial \tilde{\zeta}_0} + \tilde{U}_0 \frac{\partial \tilde{U}_0}{\partial \tilde{\zeta}_0} \right\} \right] \qquad \text{(B.2.6)}$$

$$A_2 = 3\tilde{U}_0 \left\{ \tilde{U}_0 \frac{\partial \tilde{U}_0}{\partial \tilde{\zeta}_0} + \tilde{V}_0 \frac{\partial \tilde{U}_0}{\partial \tilde{\zeta}_0} \right\} \qquad \text{(B.2.7)}$$

$$A_3 = \tilde{U}_0^3 \qquad \text{(B.2.8)}$$

and

$$B_1 = \left[\tilde{U}_0 \left(\frac{\partial \tilde{U}_0}{\partial \tilde{\zeta}_0} \right)^2 + \tilde{U}_0^2 \frac{\partial^2 \tilde{U}_0}{\partial \tilde{\zeta}_0^2} + \tilde{\bar{U}}_0^2 \frac{\partial^2 \tilde{U}_0}{\partial \tilde{\zeta}_0^2} + 2\tilde{U}_0 \tilde{\bar{U}}_0 \frac{\partial^2 \tilde{\bar{U}}_0}{\partial \tilde{\zeta}_0 \partial \tilde{\bar{\zeta}}_0} + \frac{\partial \tilde{U}_0}{\partial \tilde{\zeta}_0} \left\{ \tilde{U}_0 \frac{\partial \tilde{\bar{U}}_0}{\partial \tilde{\bar{\zeta}}_0} + \tilde{\bar{U}}_0 \frac{\partial \tilde{\bar{U}}_0}{\partial \tilde{\zeta}_0} \right\} \right] \qquad \text{(B.2.9)}$$

$$B_2 = 3\tilde{U}_0 \left\{ \tilde{U}_0 \frac{\partial \tilde{\bar{U}}_0}{\partial \tilde{\bar{\zeta}}_0} + \tilde{\bar{U}}_0 \frac{\partial \tilde{U}_0}{\partial \tilde{\zeta}_0} \right\} \qquad \text{(B.2.10)}$$

$$B_3 = \tilde{U}_0^3 \qquad \text{(B.2.11)}$$

B.3 Consider the term

$$\frac{\partial^2}{\partial \tilde{t}^2} (2\tilde{q}_x \tilde{q}_x + p_{xx}) \text{ in Eq. (2.3.6)}$$

$$\frac{\partial^2}{\partial \tilde{t}^2} (2\tilde{q}_x \tilde{q}_x + p_{xx})$$

$$= 4 \left(\frac{\partial \tilde{q}_x}{\partial \tilde{t}} \right)^2 + 4\tilde{q}_x \frac{\partial^2 \tilde{q}_x}{\partial \tilde{t}^2} + \frac{\partial^2 \tilde{p}_{xx}}{\partial \tilde{t}^2} \qquad \text{(B.3.1)}$$

where $\tilde{q}_x$ = Real part of the complex perturbation velocity $V'(\zeta)$

$\tilde{q}_y$ = Imaginary $(V'(\zeta)$

Hence we have,

$$\frac{\partial \tilde{q}_x}{\partial \tilde{t}} = \text{Re} \left(\frac{\partial \tilde{V}}{\partial \tilde{t}} \right) \qquad \text{(B.3.2)}$$

and

$$\frac{\partial^2 \tilde{q}_x}{\partial \tilde{t}^2} = \mathrm{Re}\left(\frac{\partial^2 \tilde{V}}{\partial \tilde{t}^2}\right) \tag{B.3.3}$$

Also note that,

$$\frac{\partial^2 \tilde{p}_{xx}}{\partial \tilde{t}^2} = \text{x component of } \frac{\partial^2 \tilde{p}}{\partial \tilde{t}^2} \tag{B.3.4}$$

Similarly we obtain for

$$\frac{\partial^2}{\partial \tilde{t}^2}(2\tilde{q}_x\,\tilde{q}_y) = 2\tilde{q}_x \frac{\partial^2 \tilde{q}_y}{\partial \tilde{t}^2} + 4\left(\frac{\partial \tilde{q}_x}{\partial \tilde{t}}\right)\left(\frac{\partial \tilde{q}_y}{\partial \tilde{t}}\right) + 2\tilde{q}_y \left(\frac{\partial^2 \tilde{q}_x}{\partial \tilde{t}^2}\right) \tag{B.3.5}$$

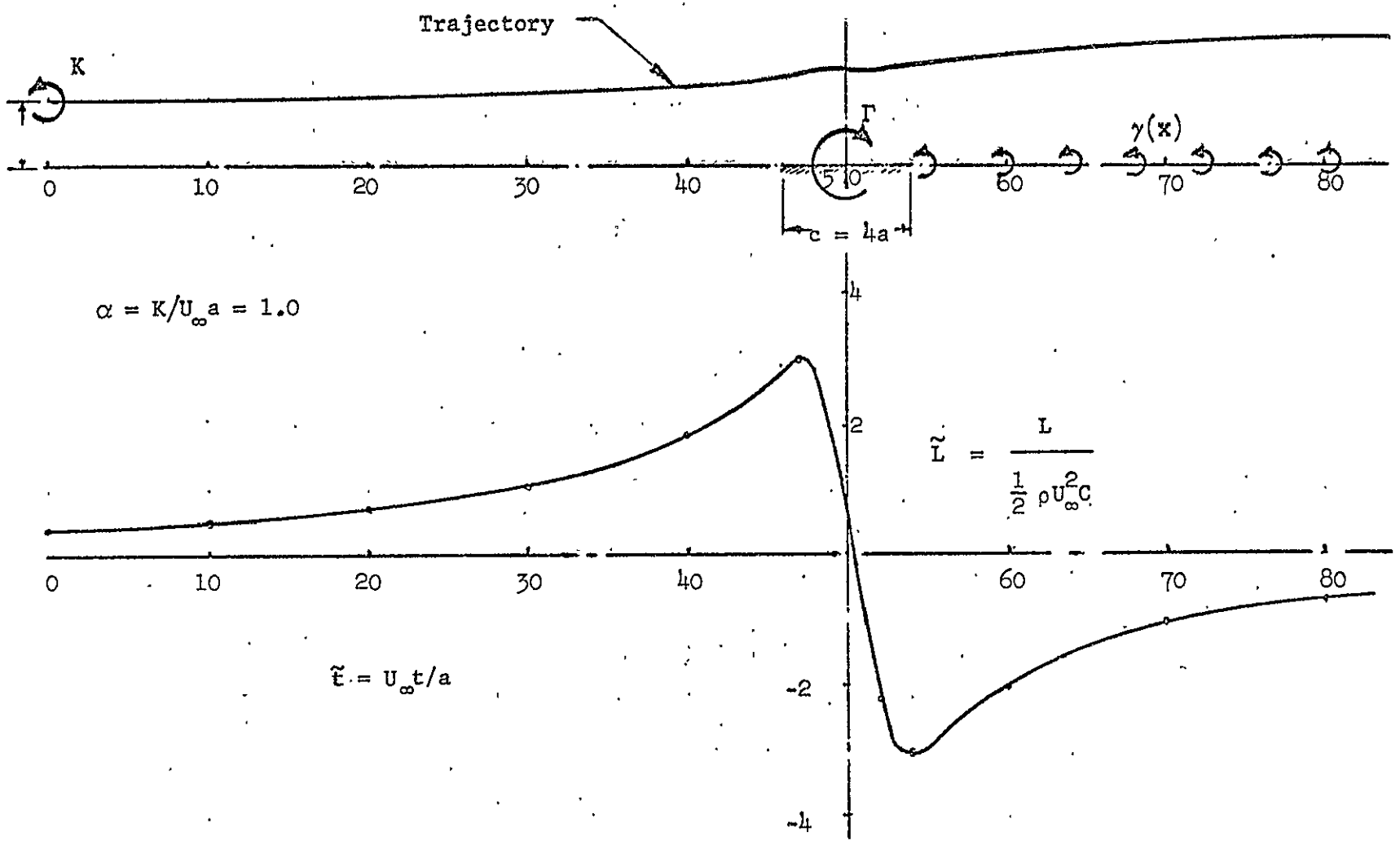

Fig. 1 -Lift force variation with time on the flat plate aerofoil.

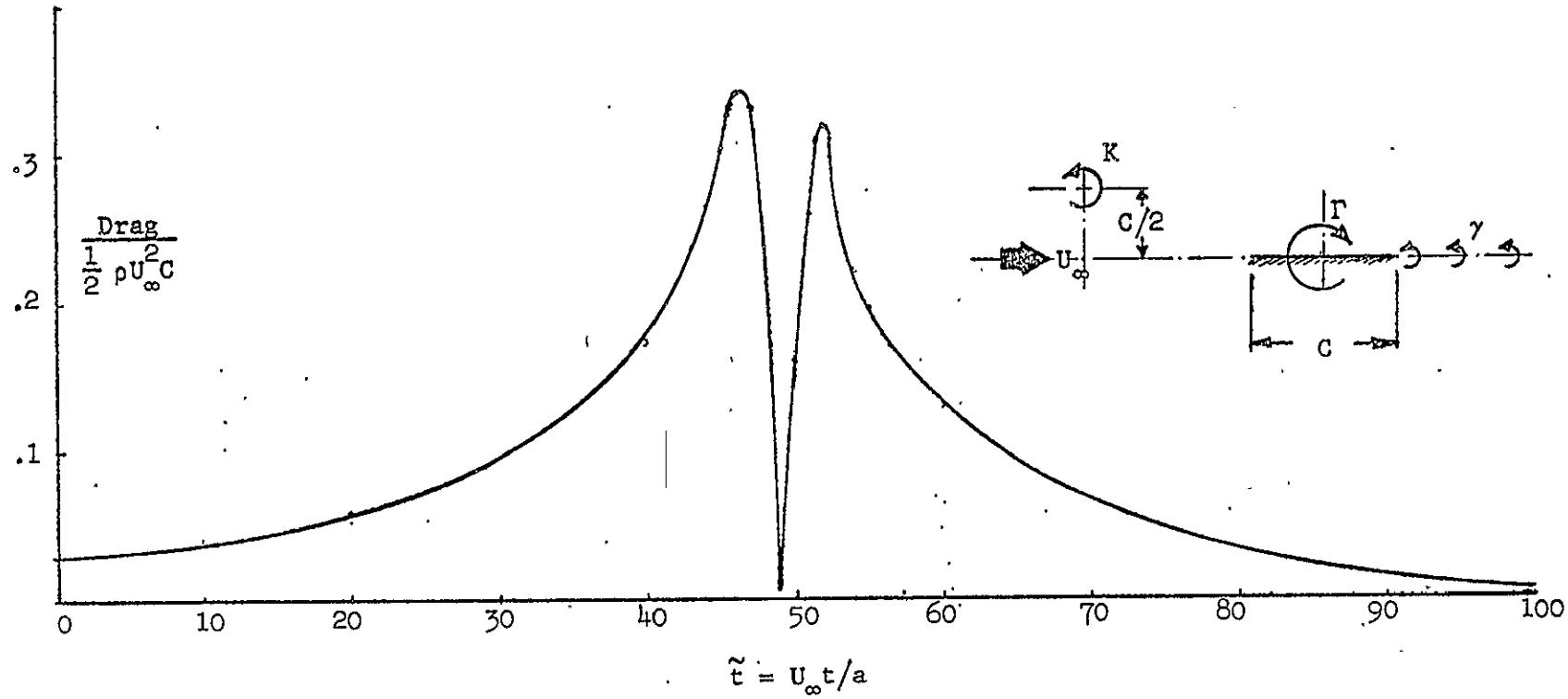

C = 4a

Fig. 2 -Drag on the plate vs vortex location.

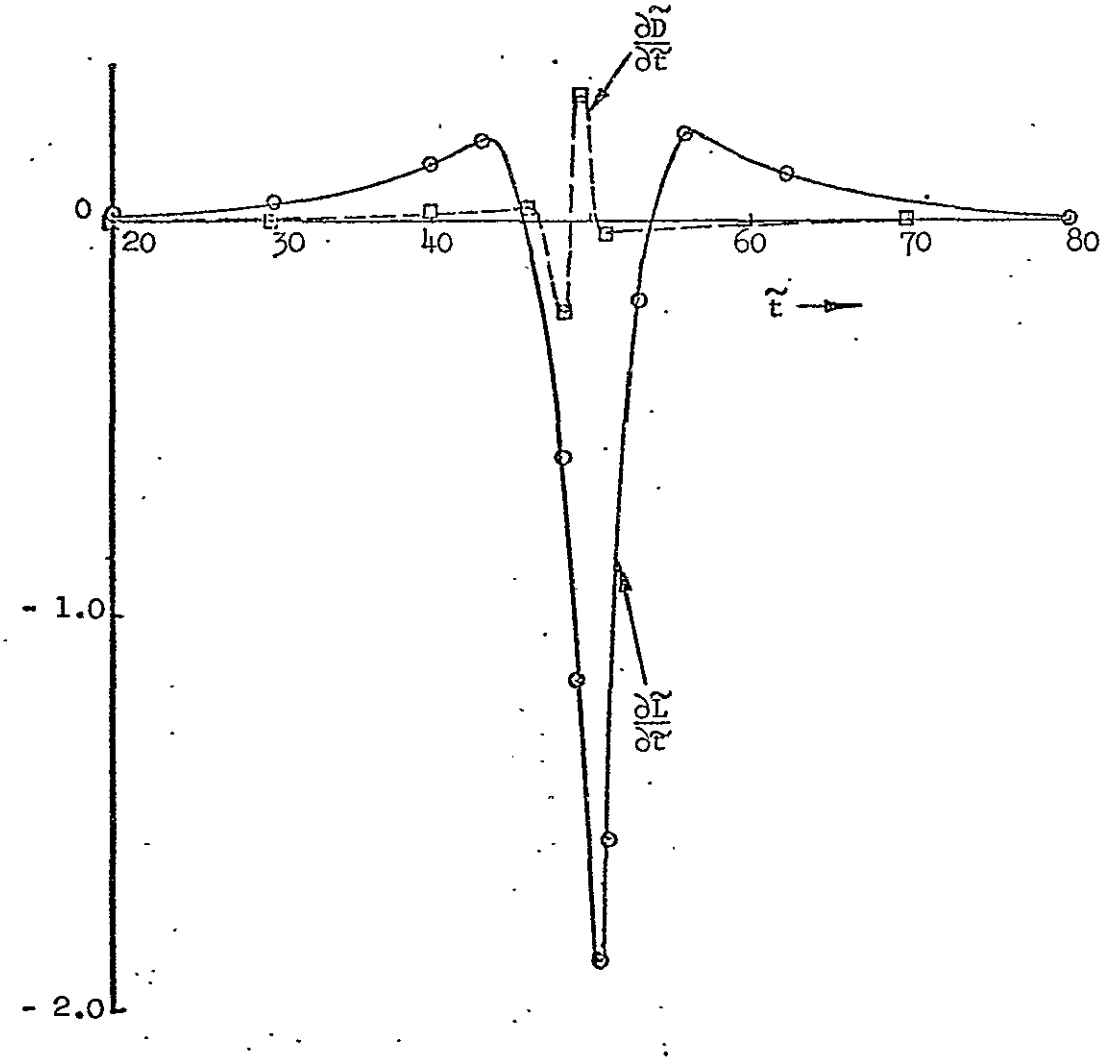

Fig. 3 --A comparison of $\partial \tilde{L}/\partial \tilde{t}$ and $\partial \tilde{D}/\partial \tilde{t}$ for vortex-flat plate interaction.

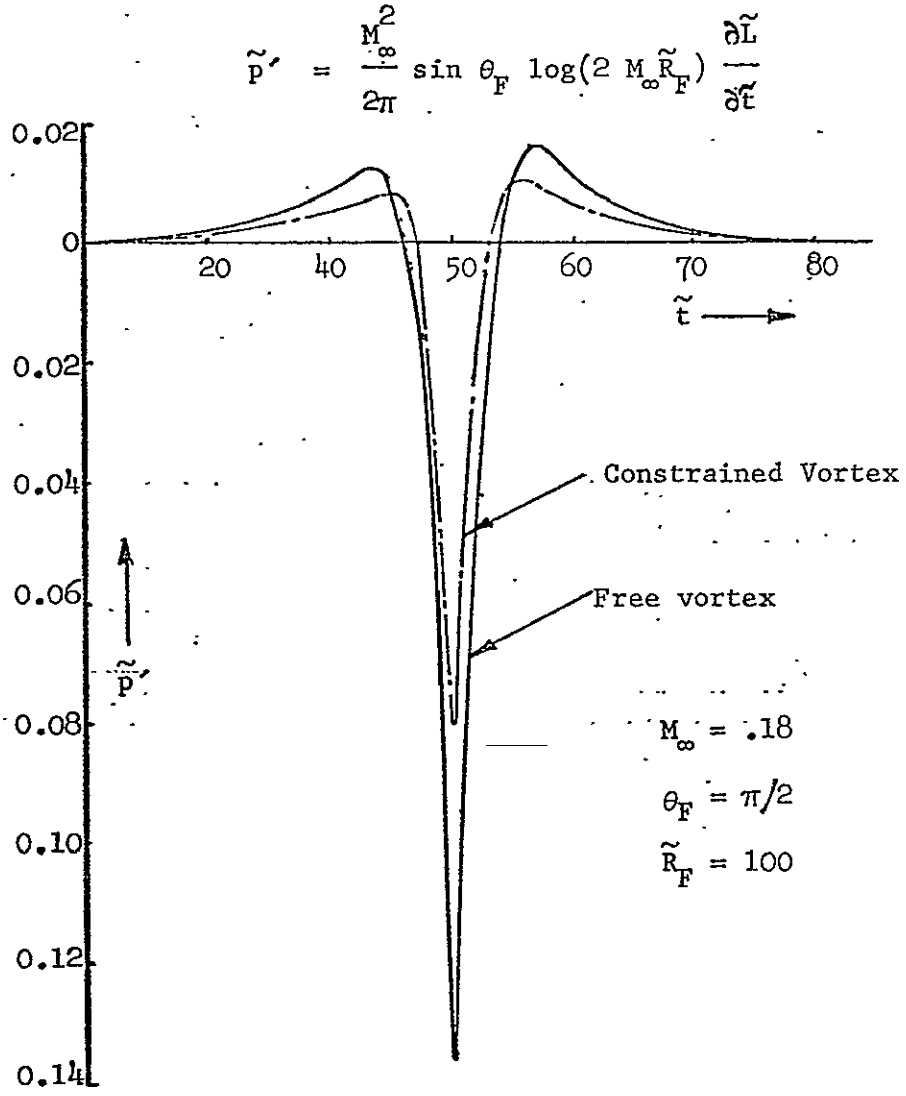

Fig. 4 --Pressure in the far field due to the lift force alone for the case of constrained and free vortex motion.

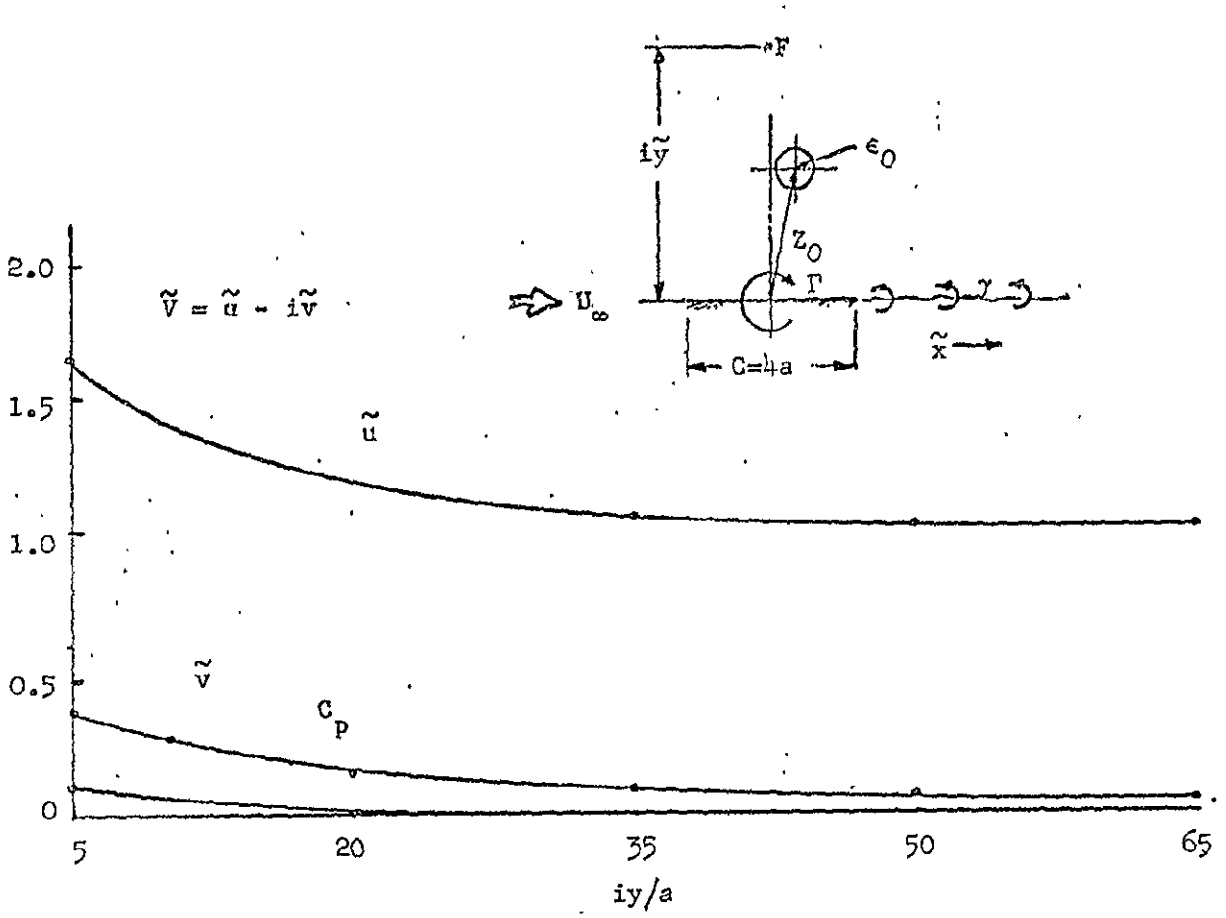

Fig. 5 --Velocity and pressure fields in the flow due to vortex-aerofoil interaction.

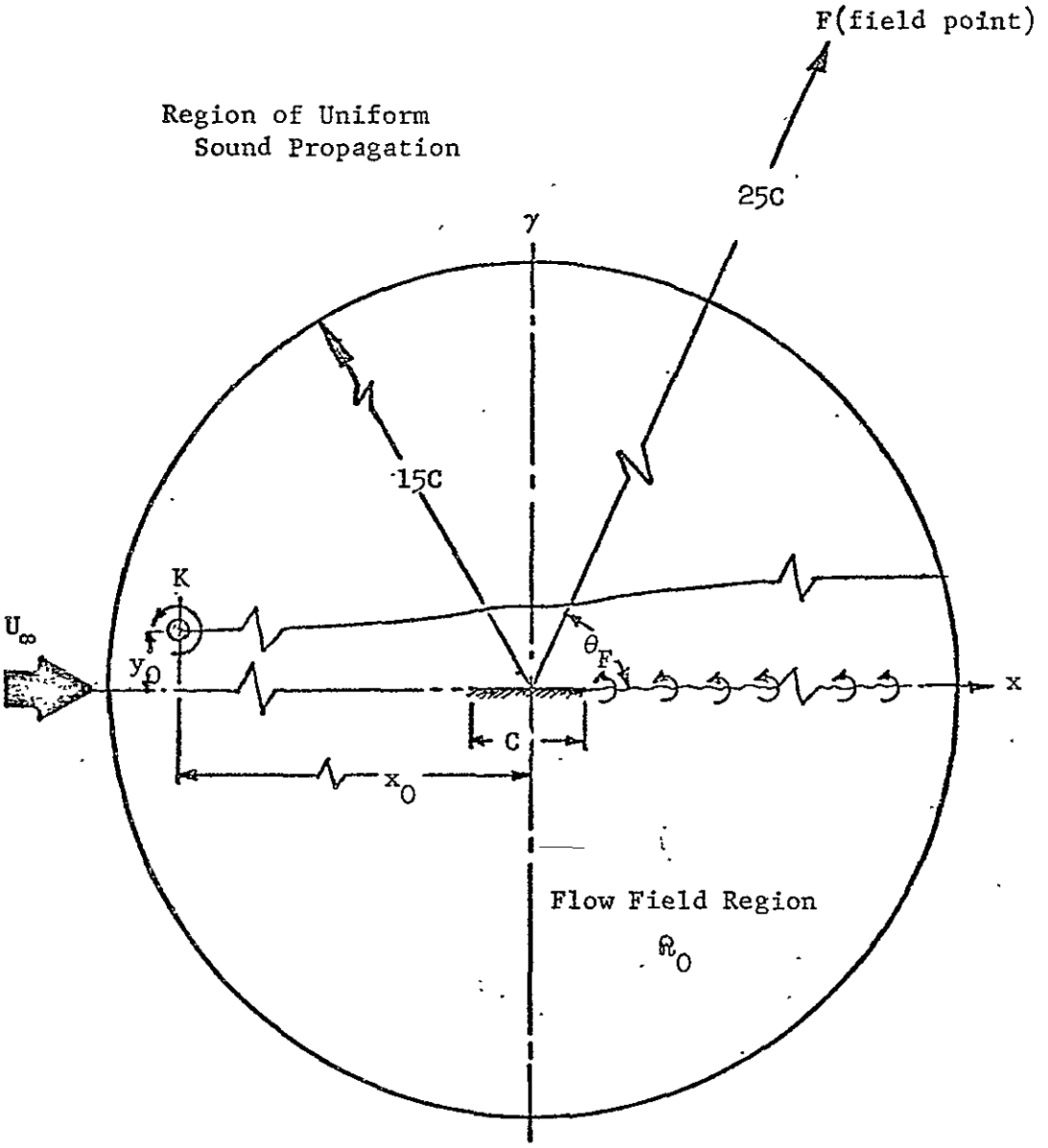

Fig. 6 -Schematic of the regions of the flow field $\mathcal{R}_0$ and the coordinates of the field point F.

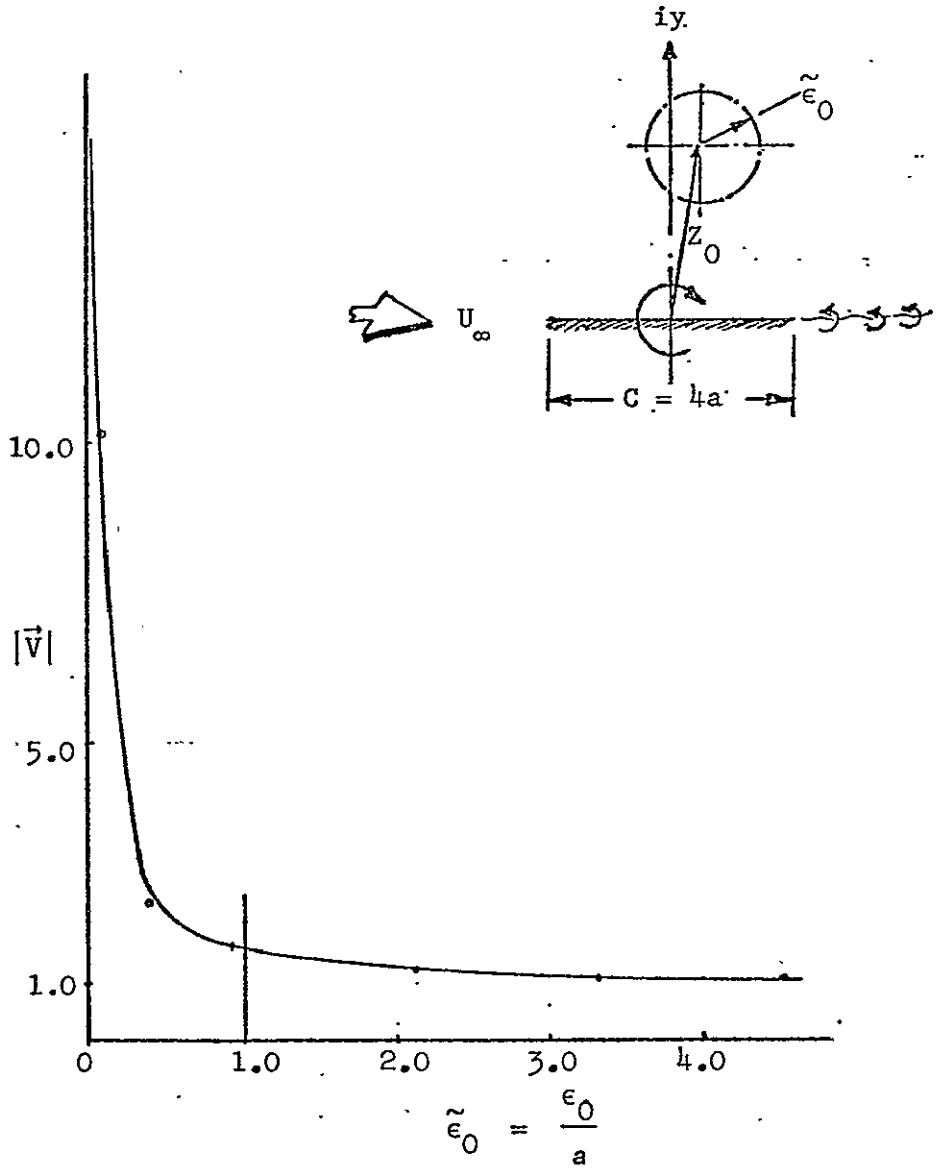

Fig. 7 -Velocity field around the vortex

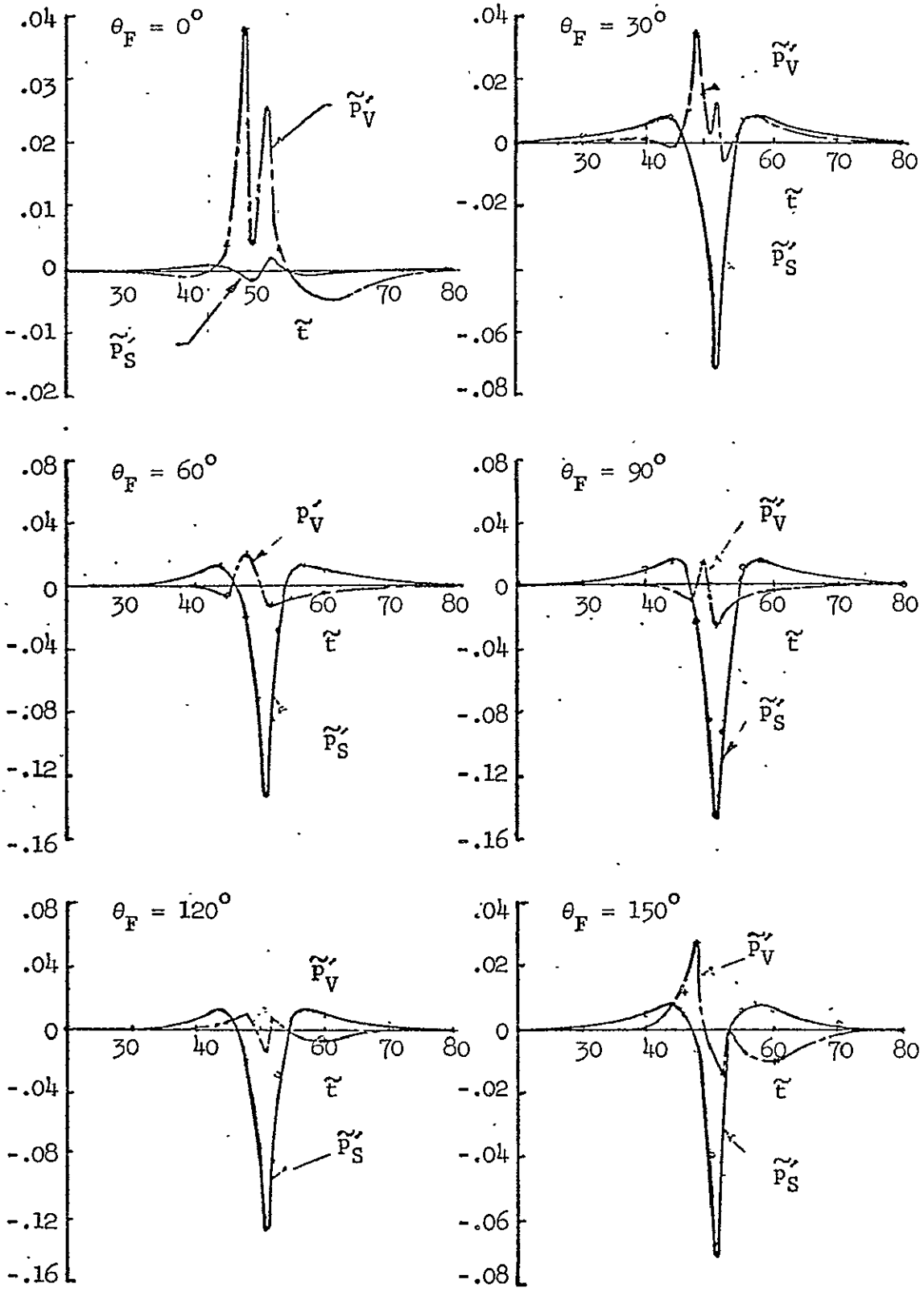

FIG. 8 (a)--Pressure in the far field due to both the quadrupoles and the dipoles as a function of angle θ_F .

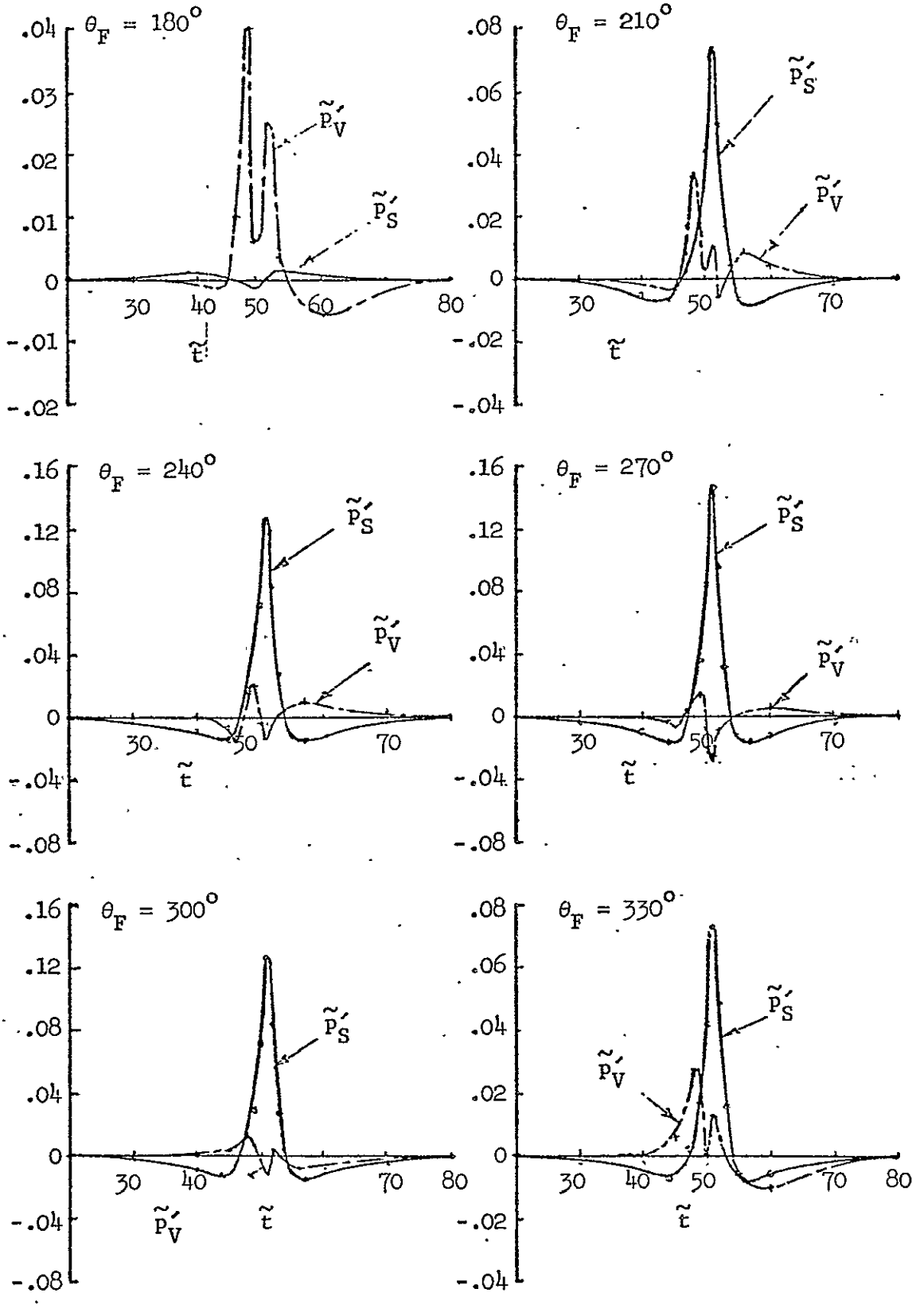

FIG. 8 (b)--Pressure in the far field due to both the quadrupoles and the dipoles as a function of angle θ_F .

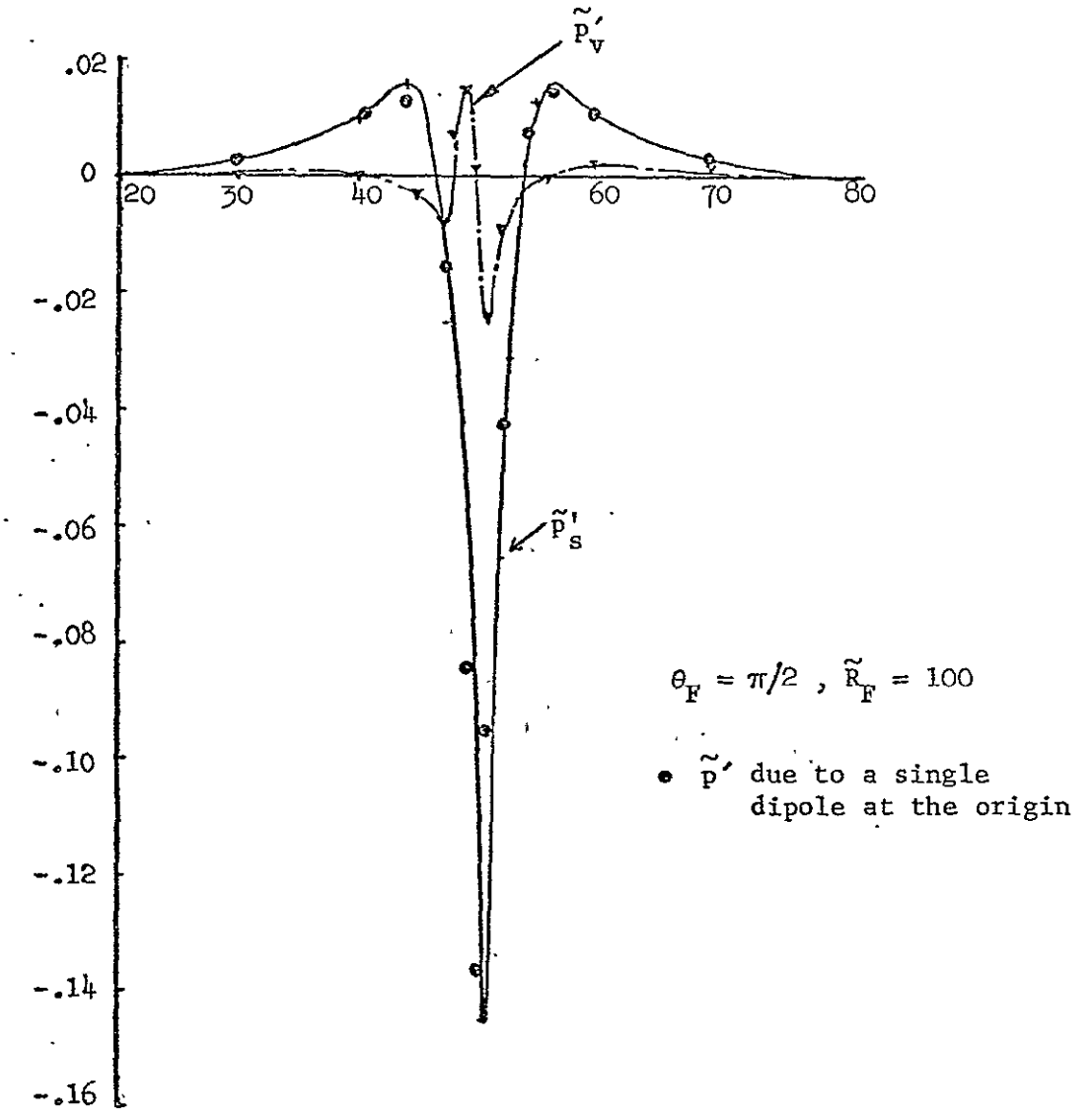

Fig. 9 --A comparison of the pressure in the far field, for $\theta_F = \pi/2$, with that due to the concentrated dipole.

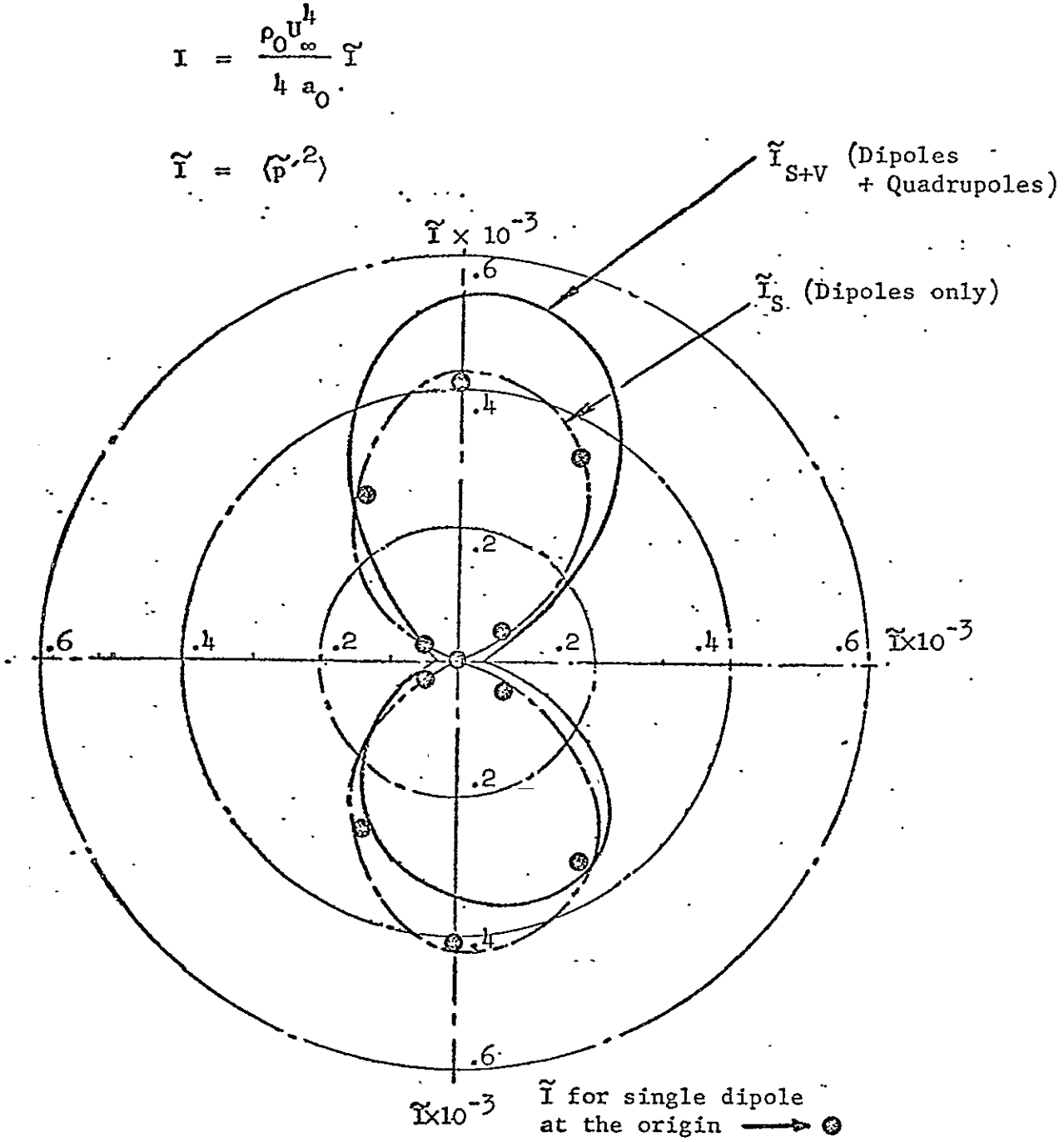

Fig.10(a)-Directivity pattern for the sound intensity in the far field for the vortex-flat plate interaction.

$$IL = 10 \log_{10}\left(\frac{I}{I_0}\right) \text{deciBels}$$

$$I_0 = 10^{-16} \text{ watts/cm}^2$$

$$\tilde{R}_F = 100, \; M_\infty = .18$$

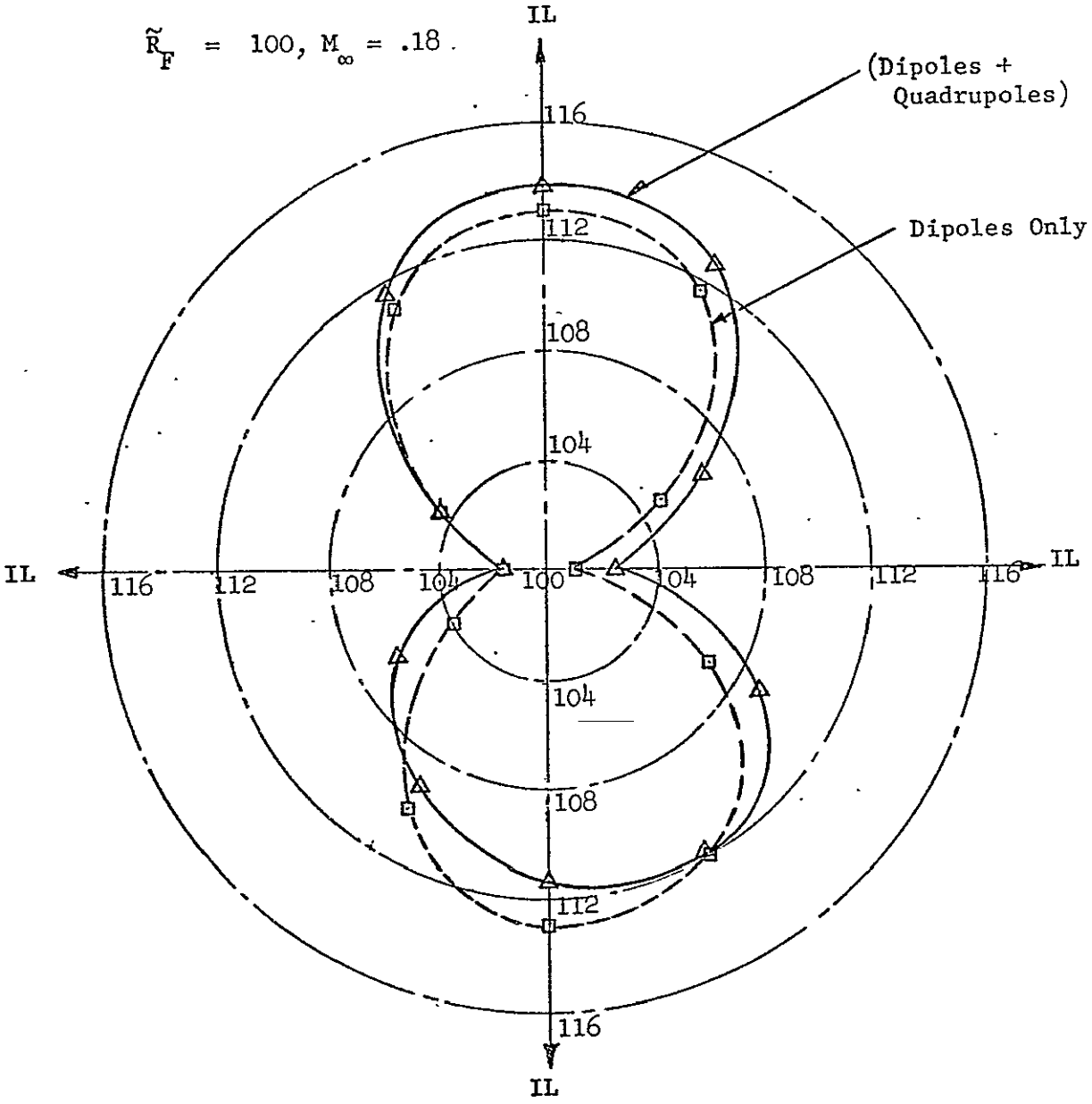

Fig. 10(b)--Intensity level in deciBels in the far field. for the vortex-flat plate interacation.

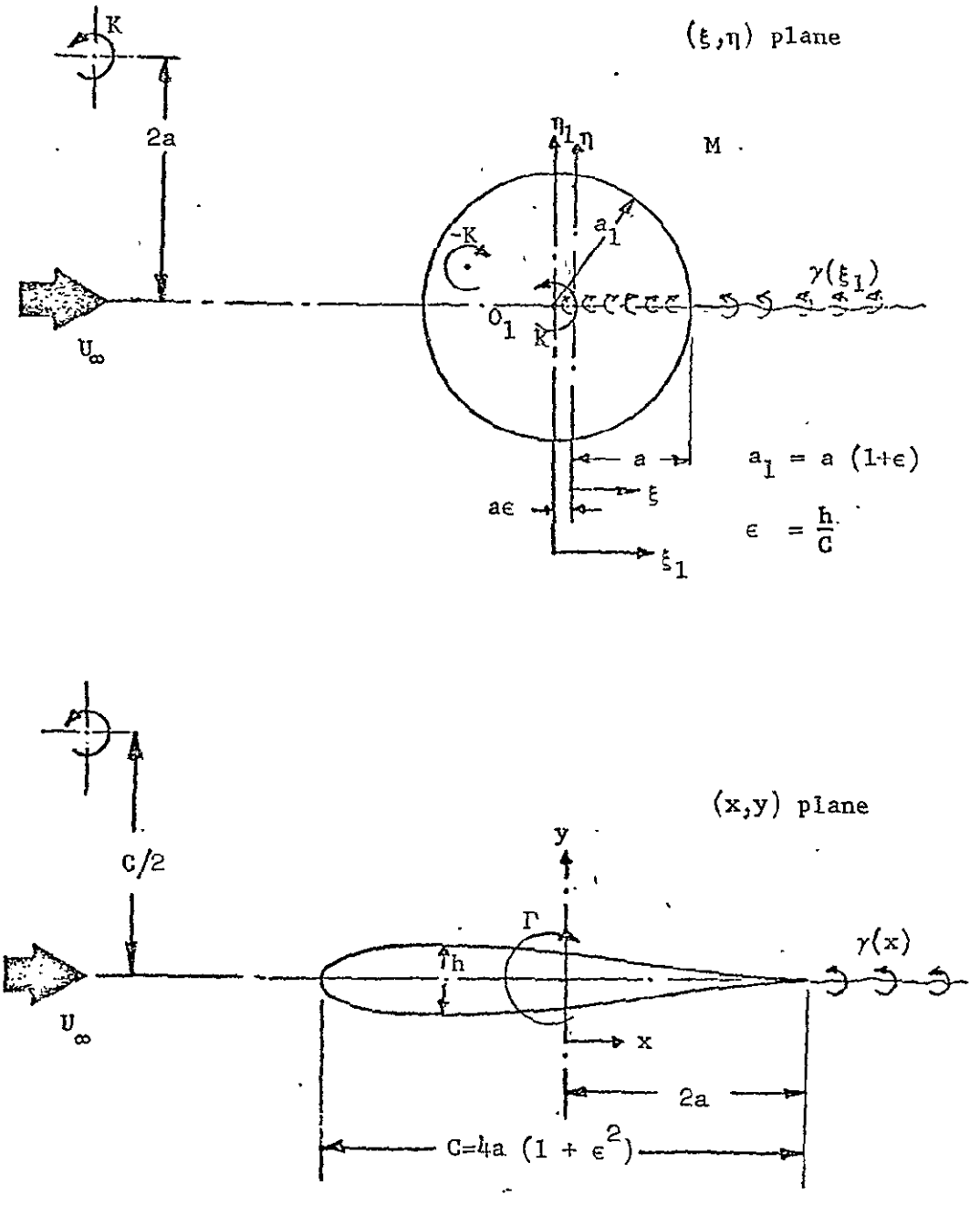

Fig. 11 -A schematic of the vortex-symmetric Jukowski aerofoil configuration.

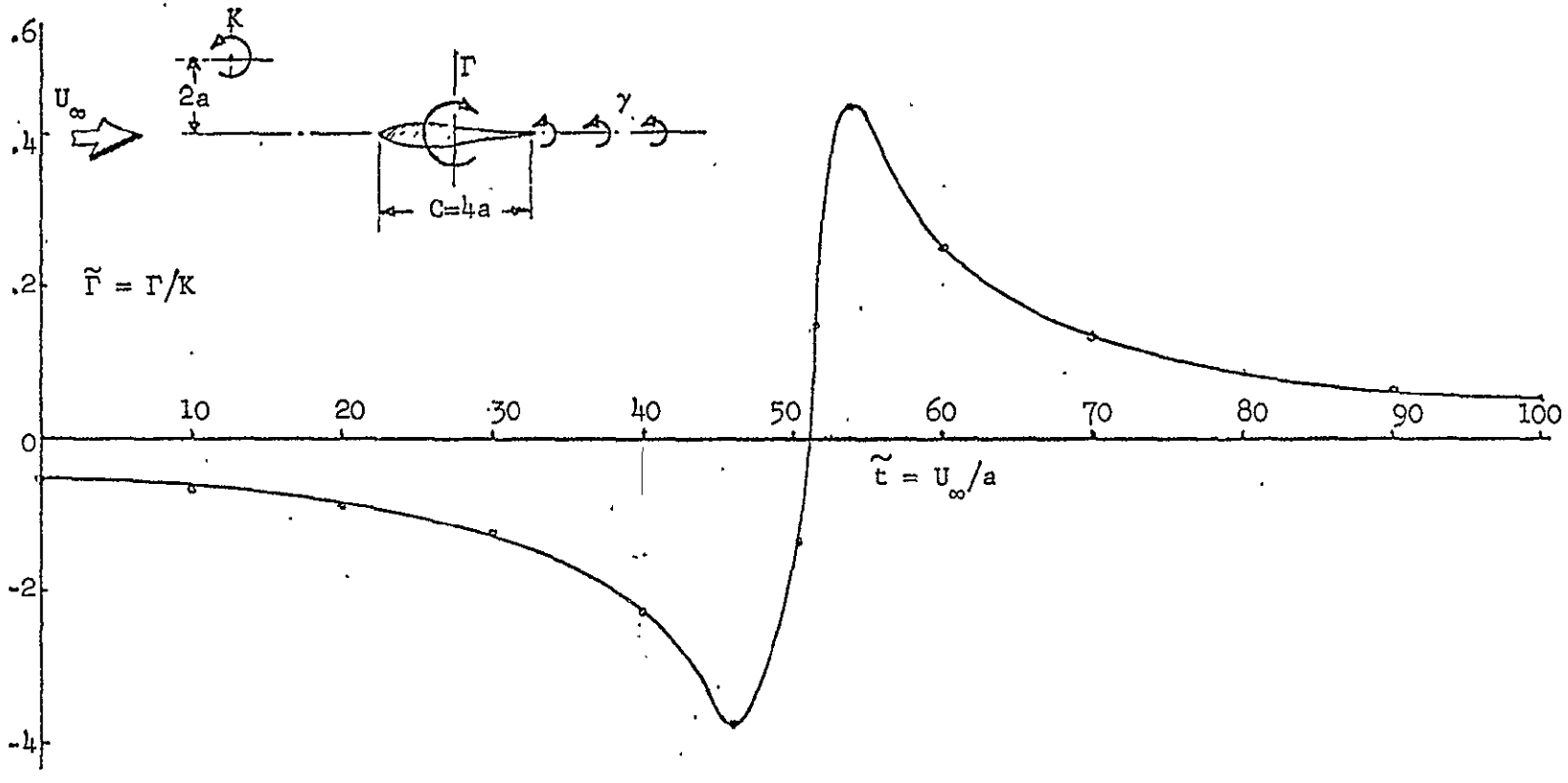

Fig. 12 -Circulation around the symmetric aerofoil as a function of time.

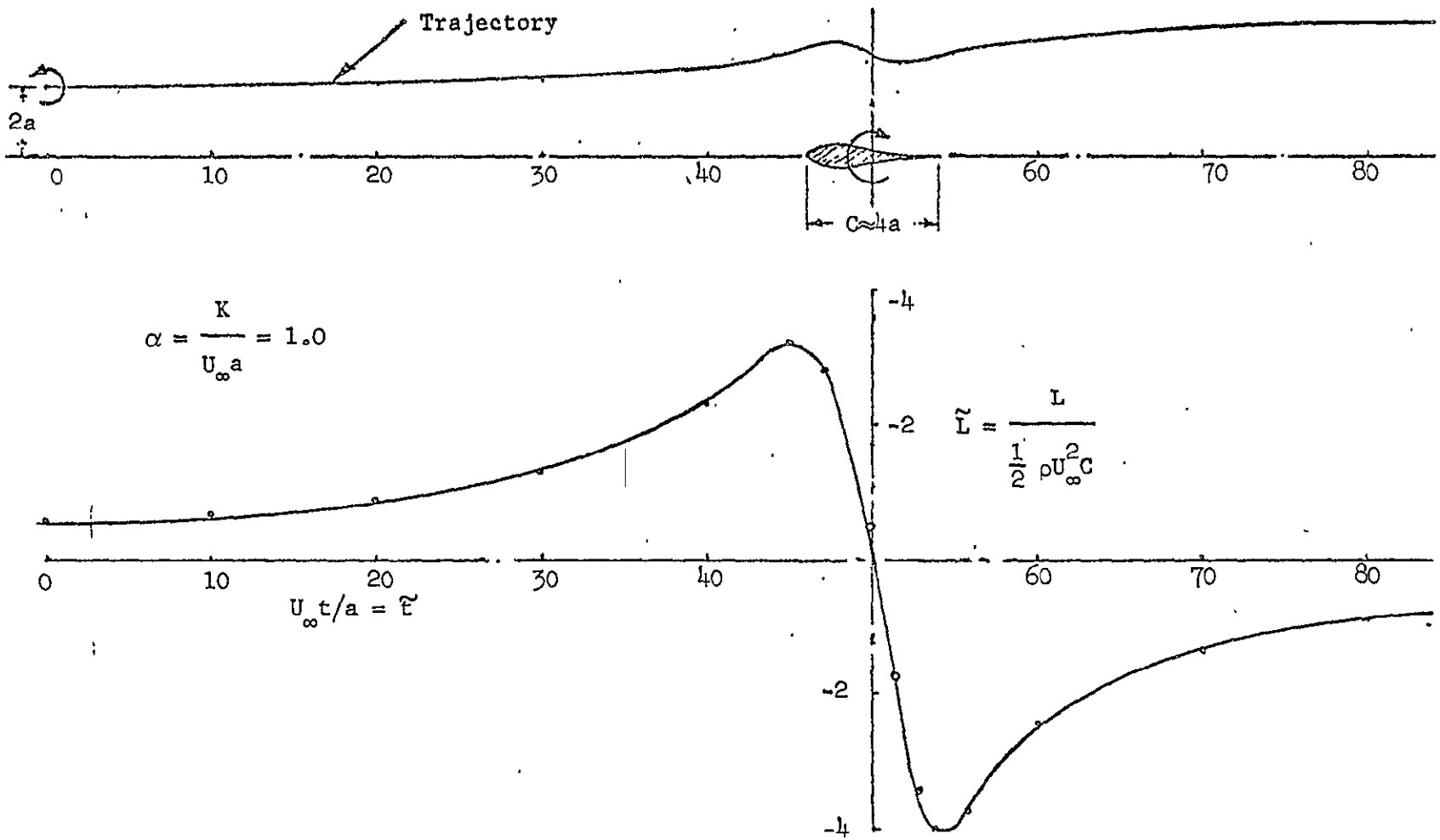

Fig. 13 -Lift variation on the symmetric aerofoil with respect to time.

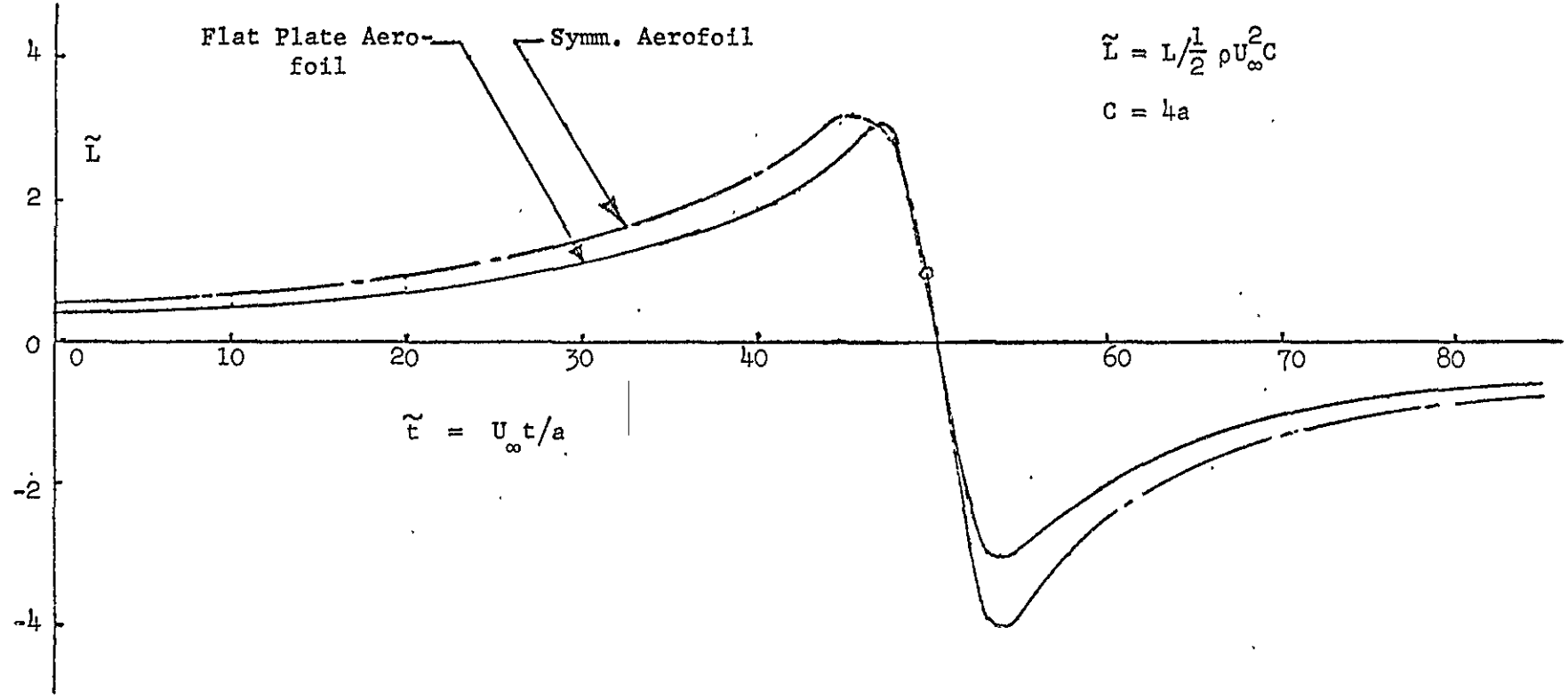

Fig. 14 -A comparison of the lift forces for the vortex-flat plate aerofoil and the vortex-symm. aerofoil.

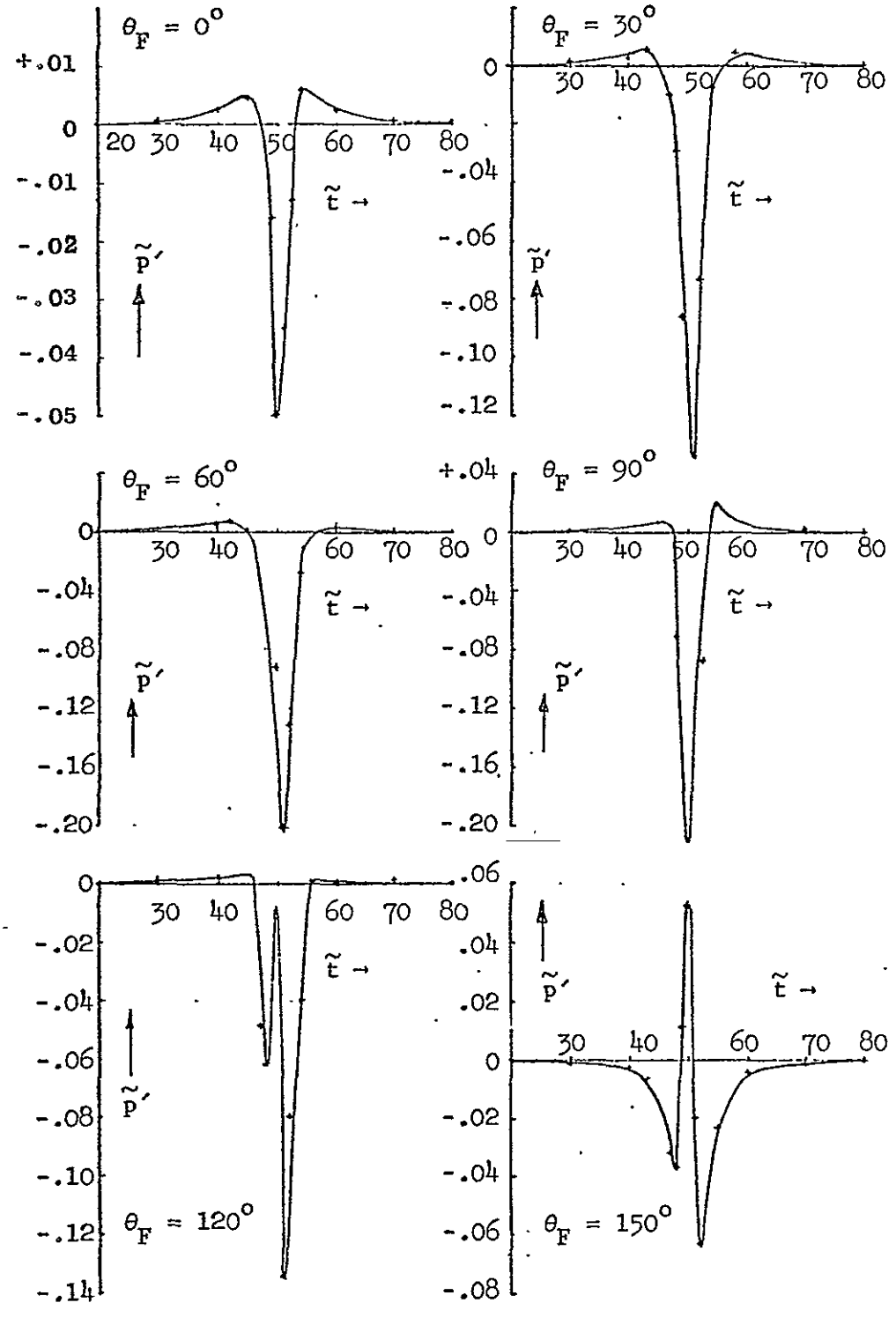

Fig. 15(a) --Pressure in the far field due to dipole distribution on the surface of symm. aerofoil.

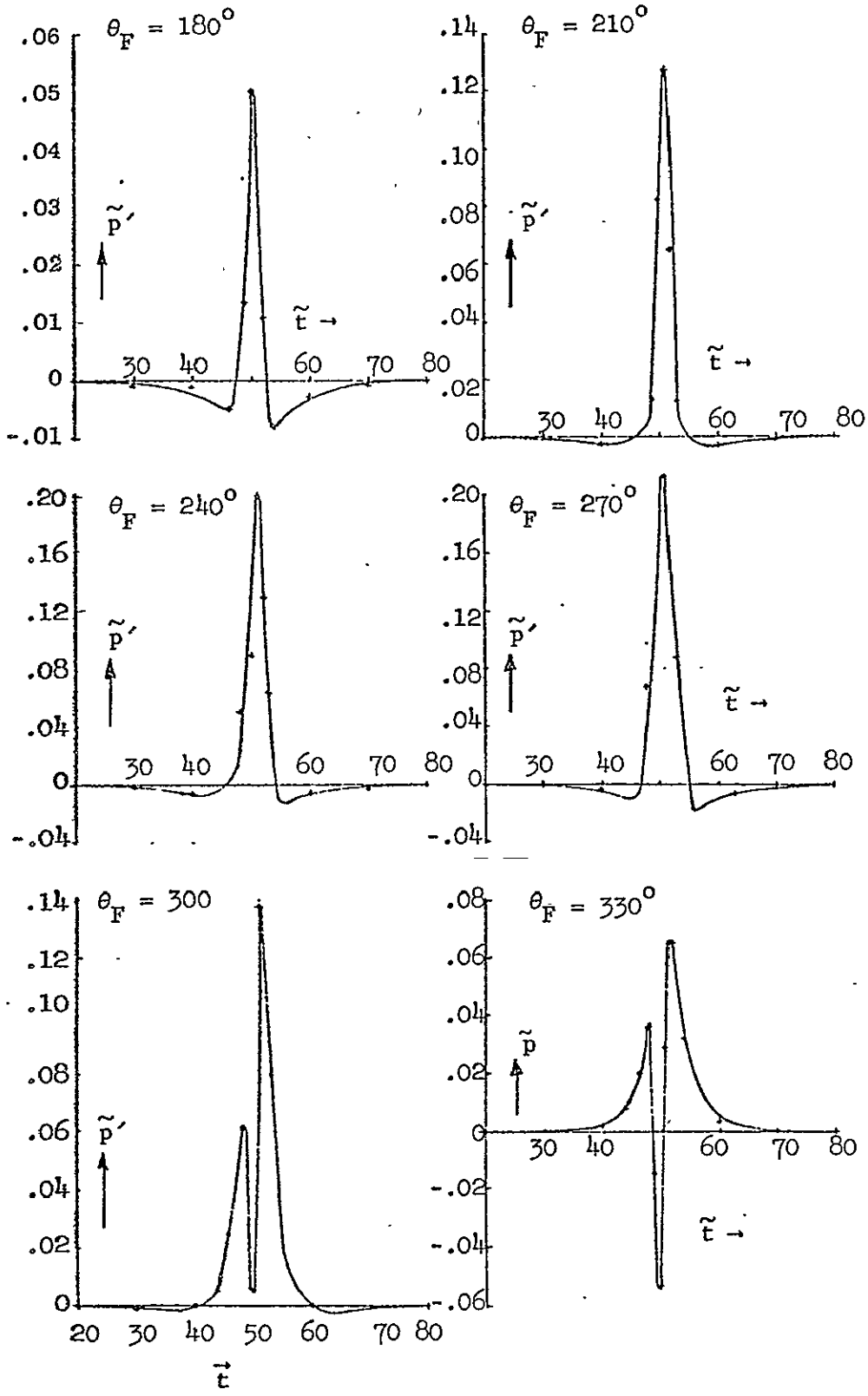

Fig. 15(b)--Pressure in the far-field due to the dipole distribution on the symmetric aerofoil surface.

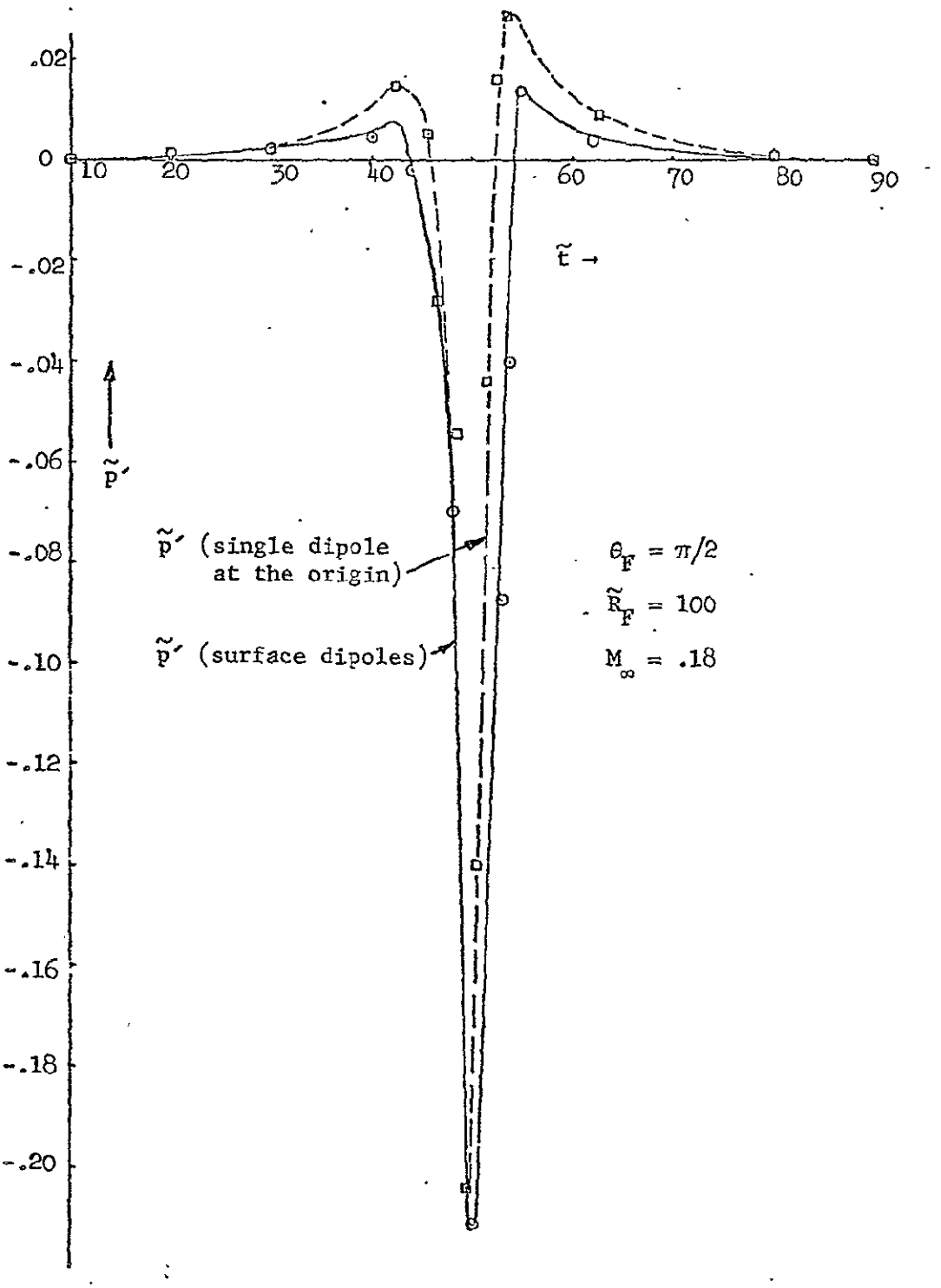

Fig. 16 -Pressure in the far-field due to the surface dipoles — a comparison with that due to a concentrated dipole for the vortex-symm. aerofoil interaction.

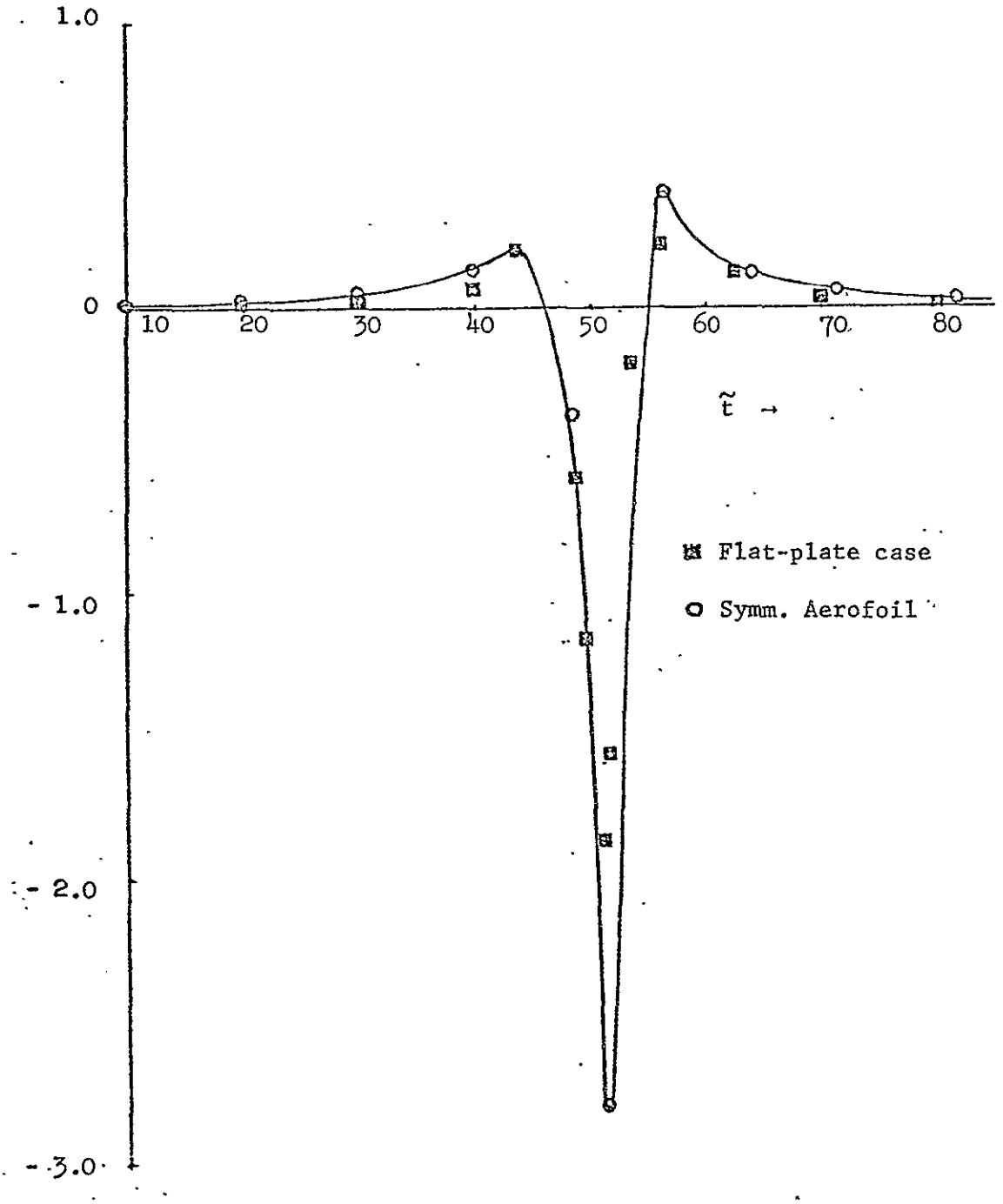

Fig. 17--Far field pressure due to a concentrated dipole – a comparison of the vortex-flat plate and vortex - symm. aerofoil interactions.

$$I = \frac{\rho_0 U_\infty^4}{4a_0} \tilde{I} \quad \text{watts/cm}^2$$

$$\tilde{I} = \langle \tilde{p}' \rangle^2$$

$$\tilde{R}_F = 100, \; M_\infty = .18$$

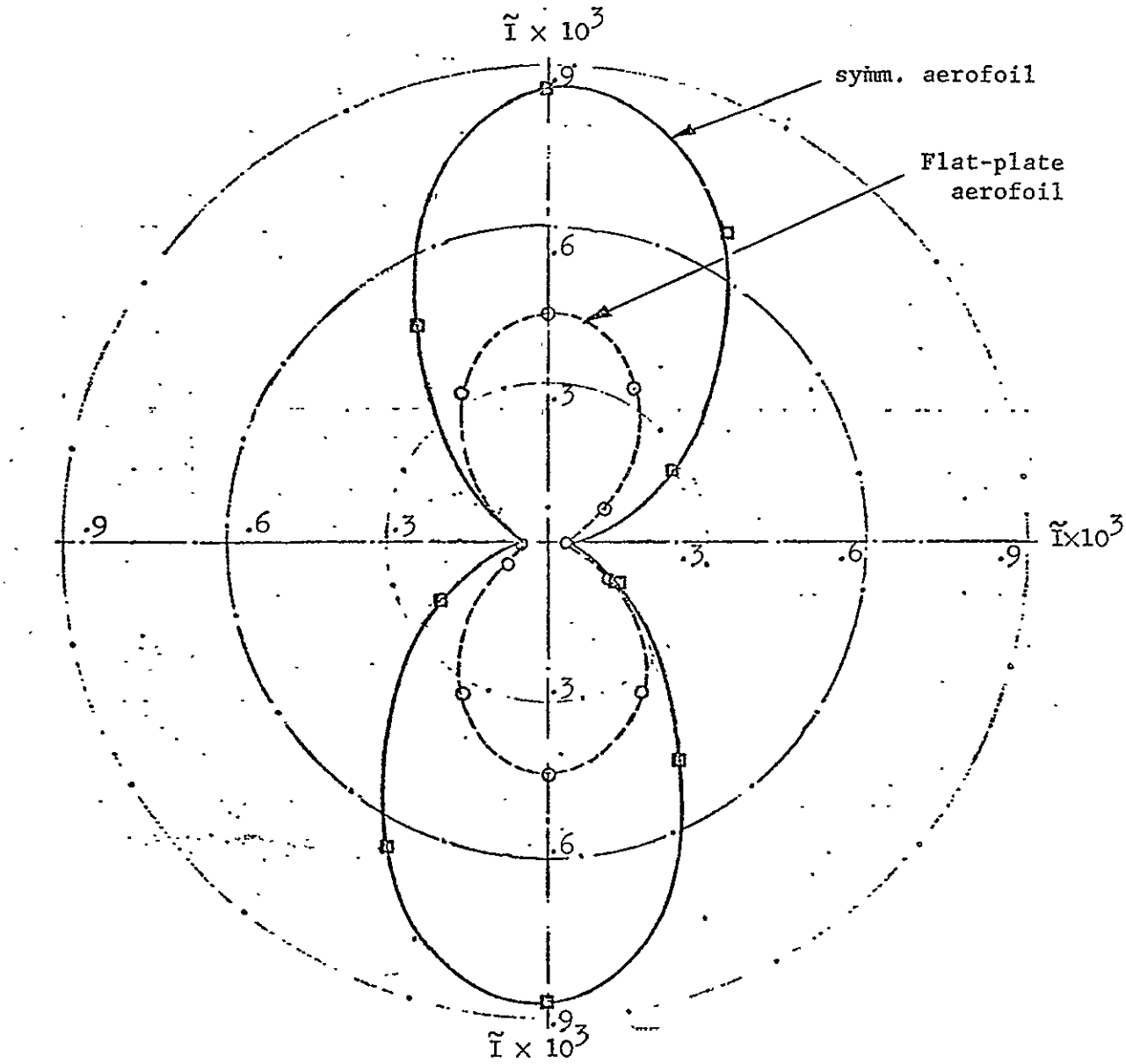

Fig. 18 -Intensity in the far-field for the vortex-symm. aerofoil interaction.

$$IL = 10 \log_{10}\left(\frac{I}{I_0}\right) \text{ deciBels}$$

$$I_0 = 10^{-16} \text{ watts/cm}^2$$

$$\tilde{R}_F = 100, \; M_\infty = .18$$

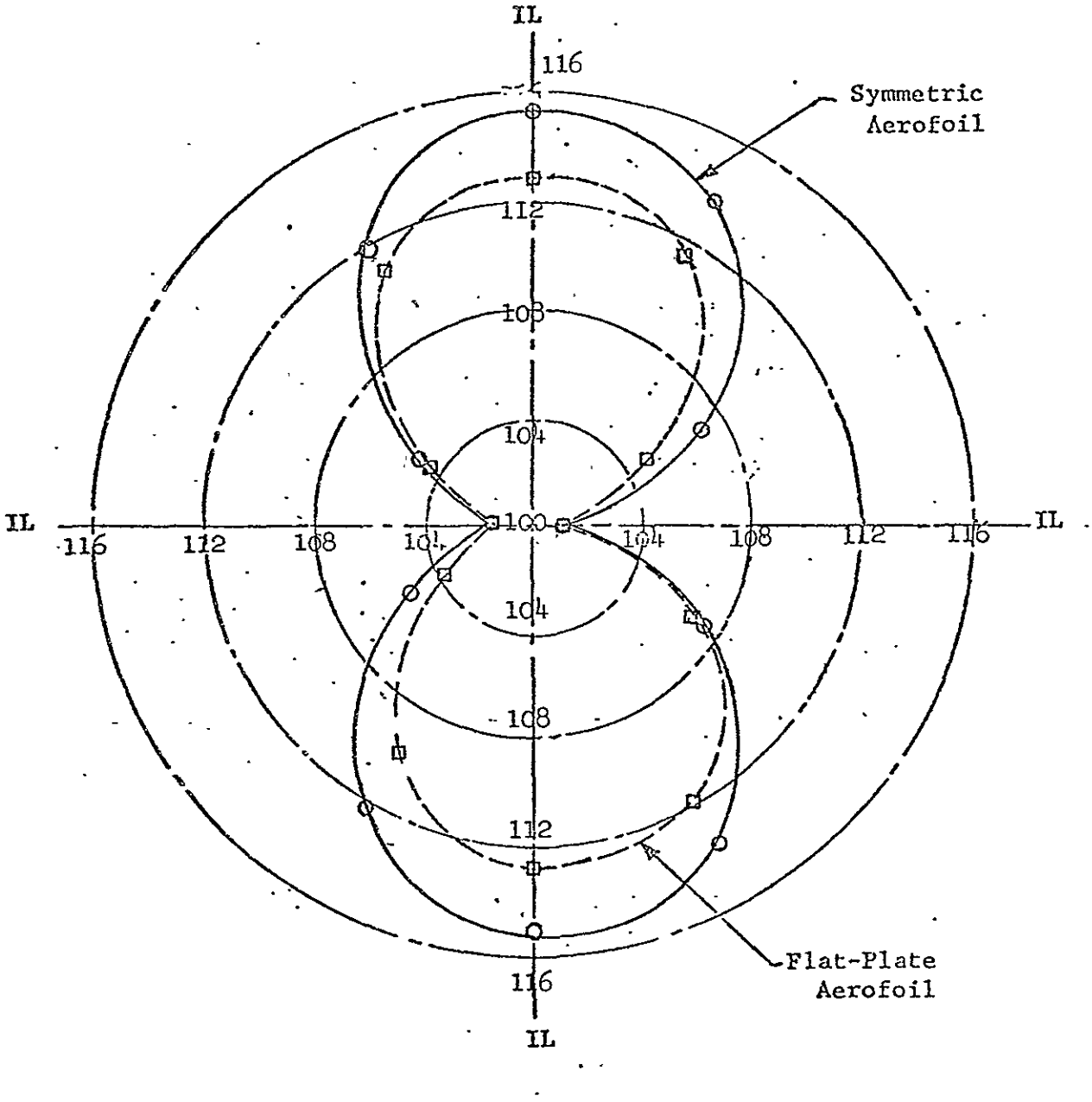

Fig. 19 -Intensity level (in deciBels) due to surface distribution of dipoles for the flat-plate and symmetric aerofoils.